Brain Structure and Function

Expression Patterns of Irx Genes in the Developing Chick Inner Ear

--Manuscript Draft--

Manuscript Number:	BSAF-D-16-00256R1
Full Title:	Expression Patterns of Irx Genes in the Developing Chick Inner Ear
Article Type:	Original Article
Keywords:	Otocyst; otic vesicle; otic specification; sensory patch; acoustic-vestibular ganglion
Corresponding Author:	Matias HIDALGO-SÁNCHEZ, Ph.D. Universidad de Extremadura SPAIN
Corresponding Author Secondary Information:	
Corresponding Author's Institution:	Universidad de Extremadura
Corresponding Author's Secondary Institution:	
First Author:	Sheila Cardeña-Núñez, Graduate
First Author Secondary Information:	
Order of Authors:	Sheila Cardeña-Núñez, Graduate
	Luis Óscar Sánchez-Guardado, PhD
	Rubén Corral-San-Miguel, Graduate
	Lucía Rodríguez-Gallardo, PhD
	Faustino Marín, PhD
	Luis Puelles, MD
	Pilar Aroca, PhD
	Matias HIDALGO-SÁNCHEZ, Ph.D.
Order of Authors Secondary Information:	

Funding Information:		
	Spanish Ministry of Science (BFU2010-19461)	PhD Matias HIDALGO-SÁNCHEZ
	Junta de Extremadura (GR10152)	PhD Matias HIDALGO-SÁNCHEZ
	MICINN (BFU2006-15530-C02/BFI)	Mrs Lucía Rodríguez-Gallardo
	Spanish Ministry of Science (BFU2005-09378-C02-01)	Mr Luis Puelles
	MICINN (BFU2014-57516P)	Mr Luis Puelles
	SENECA Foundation (19904/GERM/15)	Mr Luis Puelles
	MICINN (BFU2006-15530-C01/BFI)	Mrs Pilar Aroca
	Junta-de-Extremadura predoctoral fellowship (PRE/08031)	Mr Luis Óscar Sánchez-Guardado

Abstract:	The vertebrate inner ear is a complex three-dimensional sensorial structure with auditory and vestibular functions. The molecular patterning of the developing otic epithelium creates various positional identities, consequently leading to the stereotyped specification of each neurosensory and non-sensory element of the membranous labyrinth. The Iroquois (Iro/Irx) genes, clustered in two groups (A: Irx1, Irx2, and Irx4; and B: Irx3, Irx5, and Irx6), encode for transcriptional factors involved

	directly in numerous patterning processes of embryonic tissues in many phyla. This work presents a detailed study of the expression patterns of these six Irx genes during chick inner ear development, paying particular attention to the axial specification of the otic anlagen. The Irx genes seem to play different roles at different embryonic periods. At the otic vesicle stage (HH18), all the genes of each cluster are expressed identically. Both clusters A and B seem involved in the specification of the lateral and posterior portions of the otic anlagen. Cluster B seems to regulate a larger area than cluster A, including the presumptive territory of the endolymphatic apparatus. Both clusters seem also to be involved in neurogenic events. At stages HH24/25-HH27, combinations of IrxA and IrxB genes participate in the specification of most sensory patches and some non-sensory components of the otic epithelium. At stage HH34, the six Irx genes show divergent patterns of expression, leading to the final specification of the membranous labyrinth, as well as to cell differentiation.

Prof. Laszlo Zaborsky
Editor-in-Chief
Brain, Structure and Function

Badajoz (Spain), 11th October, 2016

Dear Professor Zaborsky,

Please find enclosed the corrected version of the manuscript (BSAF-D-16-00256), entitled: "Expression Patterns of Irx Genes in the Developing Chick Inner Ear".

Comments of the Reviewer

We have followed the referee's advice on how to improve our studies. The points that have been modified are the following:

Major comments:

"The authors show rather large differences in expression levels, even in individual sections and stages. It is surprising that they have neglected these distinctions in their summary cartoons. Why not show darker and lighter shades to depict these major differences in expression levels?"

The large differences in expression levels showed in individual sections and stages were considered in all the cartoons.

"Legend to Figure 1 states that the scale bars are 5 microns and 9 microns. This seems to be much too small, as this is close to the diameter of a single cell. The authors should recheck this. They may wish to recheck all the scale bars."

All the scale bars have been revised

Minor points:

1. "The 'short' and 'long' arrows are challenging to distinguish with so many labels and other markers. The authors might consider depicting the short arrows with some additional indicator (open arrows? Colored arrows?) to make them easier to see."

All the short arrows are now purple arrows.

2. "On page 13, the authors reference "short arrows in Fig. 3l". Should this be Fig. 2l?"

This change has been done

3. "The expression summary Figure 7 does not seem to accurately reflect the text

descriptions and the images for expression on the "lateral wall of the common crus" (page 15, line 20 and page 16 line 3). The cartoon shows expression instead on the medial wall of the common crus."
4. "Similar to point 4, I see the same discrepancy between the cartoon summary of Figure 9 and the data of Figure 9s, short arrow, for Irx3."

The expression patterns about the lateral wall of the common crus have been considered in the new versions of the cartoons.

5. "Page 15, line 23. Remove the query (?) after "heterogenous/variable"."

The (?) has been removed from the text.

6. "Figure 3 legend. Please note that the bars and letters refer to the panels of Figure 2. Same suggestion for the legends to the other summary cartoons."

This recommendation has been considered.

Looking forward to hearing from you, we trust that you will find this revised manuscript suitable for publication in *Brain, Structure and Function*. Thank you very much for your consideration.

Yours sincerely,

Matías HIDALGO-SÁNCHEZ

BRAIN, STRUCTURE, AND FUNCTION

Expression Patterns of Irx Genes in the Developing Chick Inner Ear

Sheila Cardeña-Núñez [1], Luis Óscar Sánchez-Guardado [1], Rubén Corral-San-Miguel [2], Lucía Rodríguez-Gallardo [1], Faustino Marín [2], Luis Puelles [2], Pilar Aroca [2], Matías Hidalgo-Sánchez [1,*]

[1] Department of Cell Biology, School of Science, University of Extremadura, Badajoz E06071, Spain

[2] Department of Human Anatomy and Psychobiology, School of Medicine, University of Murcia, Murcia E30100, Spain

Running head: *Irx* in the developing chick inner ear

*Correspondence to: Matías Hidalgo-Sánchez; Department of Cell Biology, University of Extremadura, Avda de Elvas s/n, 06071 Badajoz, Spain. Tel. and Fax: +34 924289411, *e-mail address:* mhidalgo@unex.es

Key words: Otocyst; otic vesicle; otic specification; sensory patch; acoustic-vestibular ganglion.

Grant sponsor: BFU2010-19461 and GR10152 (M.H.S.); BFU2005-09378-C02-01, BFU2014-51517P (with FDR fond support), SENECA 04548/GERM/06-10891, and MICINN, ISCIII, CIBER en Enfermedades Raras U736 (L.P.).

ABBREVIATIONS

ac	anterior crista
AG	acoustic ganglion
asc	anterior semicircular canal
AVG	acoustic-vestibular ganglion
bp	basilar papilla
cc	common crus
cd	cochlear duct
ect	ectoderm
ed	endolymphatic duct
es	endolymphatic sac
HB	hindbrain
hp	horizontal pouch
lc	lateral crista
lsc	lateral semicircular canal
ml	macula lagena
mn	macula neglecta
ms	macula sacculi
mu	macula utriculi
ov	otic vesicle
pc	posterior crista
psc	posterior semicircular canal
s	saccule
tv	tegmentum vasculosum
u	utricle
VG	vestibular ganglion
vp	vertical pouch

ABSTRACT

The vertebrate inner ear is a complex three-dimensional sensorial structure with auditory and vestibular functions. The molecular patterning of the developing otic epithelium creates various positional identities, consequently leading to the stereotyped specification of each neurosensory and non-sensory element of the membranous labyrinth. The *Iroquois* (*Iro*/*Irx*) genes, clustered in two groups (A: *Irx1*, *Irx2,* and *Irx4*; and B: *Irx3*, *Irx5,* and *Irx6*), encode for transcriptional factors involved directly in numerous patterning processes of embryonic tissues in many phyla. This work presents a detailed study of the expression patterns of these six *Irx* genes during chick inner ear development, paying particular attention to the axial specification of the otic anlagen. The *Irx* genes seem to play different roles at different embryonic periods. At the otic vesicle stage (HH18), all the genes of each cluster are expressed identically. Both clusters A and B seem involved in the specification of the lateral and posterior portions of the otic anlagen. Cluster B seems to regulate a larger area than cluster A, including the presumptive territory of the endolymphatic apparatus. Both clusters seem also to be involved in neurogenic events. At stages HH24/25-HH27, combinations of IrxA and IrxB genes participate in the specification of most sensory patches and some non-sensory components of the otic epithelium. At stage HH34, the six *Irx* genes show divergent patterns of expression, leading to the final specification of the membranous labyrinth, as well as to cell differentiation.

INTRODUCTION

The vertebrate inner ear is an intricate and highly asymmetric system of communicated cavities and ducts populated at discrete loci by sets of sensory cells ultimately responsible for hearing and balance functions. The otic anlage arises from a thickened portion of the cephalic ectoderm, the otic placode, that faces the developing hindbrain from rhombomere 4 down to the pro-rhombomere RhC (Sánchez-Guardado et al. 2014). This two-dimensional structure invaginates and then closes to form the otic vesicle or otocyst. The ovoid otic rudiment undergoes important morphogenetic changes that lead to its transformation into the highly complex three-dimensional inner ear structure of the adult. A key aim of developmental studies in this field is to understand the molecular and cellular mechanisms involved in the early patterning of the otic primordium. In particular, a central issue is how the diverse sensory and non-sensory epithelia are differentiated, arranged in a specific spatial pattern. This process is thought to be controlled by a network of diffusible morphogens and dynamic overlapping expression patterns of transcription factors through a multi-step mechanism (Romand et al. 2006; Abelló and Alsina 2007; Bok et al. 2007a; Fekete and Campero 2007; Ohyama et al. 2007; Sánchez-Calderón et al. 2007a; Schimmang 2007; Schneider-Maunoury and Pujades 2007; Whitfield and Hammond 2007; Kelly and Chen 2009; Frenz et al. 2010; Ladher et al. 2010; Groves and Fekete 2012; Chen and Streit 2013), which establish domains of differential fates within the developing membranous labyrinth (Fekete, 1996; Brigande et al. 2000; Fekete and Wu 2002; Sánchez-Guardado et al. 2014).

Iroquois (*Iro*/*Irx*) genes encode a family of homeodomain-containing transcription factors, which share a 13 amino acid domain (the Iro box) and an extremely conserved atypical homeodomain of the TALE (Three Amino-acid Loop Extension) super-class, as well as a small preserved C-terminal region in the protein (Bürglin 1997; Gómez-Skarmeta and Modolell 2002; Mukherjee and Büglin 2007; Kerner et al. 2009). *Iro*/*Irx* genes, found from nematodes to humans, were first discovered in *Drosophila* during mutagenesis screens designed to identify genes that affected the patterning of external sensory organs. *Drosophila* has three *Iro* genes, named *araucan* (*ara*), *caupolican* (*caup*), and *mirror* (*mirr*), which form the *Iroquois* complex (Iro-C) (Gómez-Skarmeta et al. 1996; McNeill et al. 1997; Ikmi et al. 2008; reviewed by Cavodeassi et al. 2001; Gómez-Skarmeta and Modolell 2002). In most vertebrates, the *Irx* family is composed of six genes, organized into two clusters, IrxA (*Irx1*, *Irx2*, and *Irx4*) and IrxB (*Irx3*, *Irx5* and *Irx6*), and located in two different chromosomes (Peters et al. 2000; Mummenhoff

et al. 2001; Ogura et al. 2001; Gómez-Skarmeta and Modolell 2002). In some other vertebrates, like zebrafish for instance, 11 *Irx* genes are organized in four clusters (Dildrop and Rüther 2004; Feijóo et al. 2004). In *C. elegans* only a single IRO gene is present, *irx-1* (Mukherjee and Bürglin 2007). *Irx* genes have also been recognized in a few other species (Perovic et al. 2003; Mukherjee and Bürglin 2007; Irimia et al. 2008; Larroux et al. 2008; Kerner et al. 2009). The evolution of these *Irx* genes is consistent with cluster duplications of an ancestral three-member cluster with an apparently conserved genomic organization, suggesting a common mechanism for the regulation of their expression patterns and extensive functions during embryonic development (Peters et al. 2000; Cavodeassi et al. 2001; Gómez-Skarmeta and Modolell 2002). Further sequence and functional comparison of *Irx* enhancers will be needed to decide whether the regulatory parallelism has a common ancestry, or originated independently in metazoans (Cavodeassi et al. 2001; Gómez-Skarmeta and Modolell 2002; Kerner et al. 2009).

Members of the *Irx* family seem to be pivotal factors in patterning and cell specification during development either as activators or repressors; this dual function depends on the *Irx* gene considered and the species under study. *Irx* genes are initially expressed in large territories, but restrict afterwards their expression to smaller subdomains. New domains of expression also can appear late during development, being required for additional patterning activities (Cavodeassi et al. 2001; Mummenhoff et al. 2001; Gómez-Skarmeta and Modolell 2002). In *Drosophila*, it has been shown that these genes act as pre-patterning genes controlling the specification of the identity of the body-wall and wing (Gómez-Skarmeta et al. 1996; McNeill et al. 1997; Kehl et al. 1998; Diez-del-Corral et al. 1999; Ikmi et al. 2008; reviewed in Cavodeassi et al. 2001; Calleja et al. 2002). In vertebrates, numerous *Iro*/*Irx* expression patterns have been studied in several developing systems (limb: Houweling et al. 2001; Zülch et al. 2001; Lebel et al. 2003; lung: Becker et al. 2001; gonad: Jorgensen and Gao 2005; and kidney: Lebel et al. 2003; Reggiani et al. 2007; reviewed in El-Dahr et al. 2008). In the developing heart, *Irx* genes exhibit expression patterns that are very much chamber-specific (Bao et al. 1999; Bruneau et al. 2001; Christoffels et al. 2000; Mummenhoff et al. 2001; Joseph 2004; Constantini et al. 2005; López-Sánchez et al. 2010; Gaborit et al. 2012; reviewed by Kim et al. 2012). In the developing central nervous system, *Irx* genes are directly involved in the early specification of various neural territories and their later anteroposterior and dorsoventral subdivisions (see Discussion).

Studies of fate specification have revealed that *Irx* genes present a coordinated cluster-specific regulation (Peters et al. 2000; Cavodeassi et al. 2001; Feijóo et al. 2004; de la Calle-Mustienes et al. 2005; Tena et al. 2011). Thus, the expression patterns of *Irx1* and *Irx2* (cluster A) are almost identical in several tissues during development, and this is also true for *Irx3* and *Irx5* (cluster B). The expression patterns of the third gene in each cluster (*Irx4* or *Irx6*) are, in general, more divergent. In some tissues, however, all the genes of a cluster, or even of both clusters, are expressed identically. This suggests that some enhancers act on all *Irx* genes of a cluster and that some of these enhancers control both clusters (Gómez-Skarmeta and Modolell 2002). Moreover, in some tissues the paralogues (*Irx1*/*Irx3* and *Irx2*/*Irx5*) are expressed identically, suggesting duplications of specific regulatory elements (Gómez-Skarmeta and Modolell 2002). Thus, *Irx* context-dependent functions could be mediated by an intricate network of different signaling pathways (Cavodeassi et al. 2001; Mummenhoff et al. 2001; Gómez-Skarmeta and Modolell 2002). Further studies have to be performed to better understand possible partial redundancies (Gómez-Skarmeta et al. 1996, 1998; Cavodeassi et al. 2001; Lebel et al. 2003).

Some descriptive studies have focused previously on the expression patterns of *Irx* genes in the developing inner ear of *Xenopus* and mouse (Bosse et al. 1997; Goriely et al. 1999; Mummenhoff et al. 2001; Rodríguez-Seguel et al. 2009). In chick, an *Irx* signaling pathway seems to be required for the maintenance of proneural and non-neural identities at the otic cup stage (Abelló et al. 2007). Chick *Irx2* expression was detected in a small area in the lateral wall of the otic anlage at the HH15-16 stage (Goriely et al. 1999). However, the detailed expression patterns of *Irx* genes in the vertebrate inner ear remain unknown. To gain insight into the possible role of *Irx* genes in different phases of chick inner ear development, we carried out a comprehensive *in situ* hybridization study of the spatiotemporal expression patterns of these genes from the otic vesicle stage (stage HH18-20) to 8 embryonic days *in ovo* (stage HH34; Hamburger and Hamilton 1951). We compared these expression patterns with *Fgf10* gene signal, which is an excellent marker for all sensory patches in the developing chicken inner ear (Sánchez-Guardado et al. 2013). At the otic vesicle stage, HH18, our detailed study shows that the expression patterns of Irx genes of cluster A (*Irx1* and *Irx2*) and cluster B (*Irx3*, *Irx5*, and *Irx6*) both seem to govern the specification of the lateral and posterior aspects of the otic anlage, with cluster B extending over a larger area than cluster A(it includes the presumptive territory of the endolymphatic apparatus) . As development proceeds (HH24/25-HH27 stages), dynamically changing and heterogeneous expression

patterns of the IrxA and IrxB genes suggest that a combination of these genes participates in the specification of several sensory patches as well as some non-sensory components of the otic epithelium. At stage HH34, each *Irx* gene showed an unique distribution compared to other members of its cluster, contributing to final differential specification of the membranous labyrinth, as well as to cell differentiation events. With the exception of *Irx4*, *Irx* genes possibly contribute to neurogenic processes forming the acoustic and vestibular ganglia. Consequently, the present study provides descriptive evidence for a direct involvement of *Iro*/*Irx* genes in the patterning of the chick otic epithelium, in all probability generating differential positional identities. The possible relationship of *Irx* genes with the network of several other signals controlling the patterning, morphogenesis, and specification of the otic anlage (such as FGF, WNT, BMP, and retinoic acid morphogens) will be discussed. Our investigation may underpin further experimental studies aimed at understanding the role of transcription factors and signaling pathways in the developing inner ear.

MATERIALS AND METHODS

Processing of the tissue

Chick embryos were obtained from fertilized White Leghorn chick eggs incubated in a humidified atmosphere at 38°C. All embryos were treated according to the recommendations of the European Union and the Spanish government for laboratory animals. Embryos ranging between stages HH20 and HH41 (Hamburger and Hamilton 1951) were fixed by immersion in 4% paraformaldehyde in 0.1 M phosphate buffered saline solution (PBS; pH 7.4), at 4°C overnight (eventually after intracardiac perfusion with the same solution). The fixed embryos were rinsed and cryoprotected in 10% sucrose solution in PBS, and were then embedded in the same buffered sucrose solution with added 10% gelatin. The blocks were frozen for 1 minute in isopentane cooled to -70°C by dry ice, and then stored at -80°C. Cryostat serial sections 20 µm-thick were cut in the transverse and horizontal planes, mounted as parallel sets on SuperFrost slides, and stored at -80°C until use. Twenty embryos were used per stage.

Cloning and synthesis of riboprobes

Genomic DNA was extracted from fresh limb buds of embryos at stage HH35-36. The tissue was incubated for 2 h at 37°C in 200 µl lysis buffer (100 mM Tris-HCl, pH 8.0; 1 mM EDTA; 250 mM NaCl; 0.2% SDS; 0.25 mg/ml Proteinase K). The solution was centrifuged at 12 000 rpm for 15 minutes at room temperature. The same volume (200 µl) of chloroform:isoamyl alcohol was then added to the supernatant, which was gently agitated, and the mixture centrifuged at 12 000 rpm for 5 minutes at room temperature. After this step, 200 µl of chloroform were added to the supernatant and centrifugation proceeded in the same way. To precipitate the DNA, we added absolute ethanol (2 volumes) and sodium acetate buffer pH 5.2 (0.1 volumes). The solution was incubated for 2 h at -20°C and then centrifuged at 12 000 rpm for 30 minutes at 4°C. The pellet was suspended again in 200 µl 70% ethanol, followed by centrifugation in the same way for 10 minutes. Finally, the pellet was suspended again in 10 µl of Sigma water.

The resulting DNA was used as a template for PCR, which was performed with Taq polymerase (M8305, Promega, Madison, WI) and specific primers for *Irx3* (forward primer: 5´-gccgccttcccgcaccacca-3´, reverse primer: 5´-gccgtaggagttgccctcctc-3´), *Irx5* (forward primer: 5´-gcagtgccccttccccaacg-3´, reverse primer: 5´-gaaccgaagcacagtcccagc -3´), and *Irx6* (forward primer: 5´-tacgggccggtggacttcacc-3´,

reverse primer: 5´-tcctgtcccgccctgccctac-3´) genes. These primer pairs were designed to flank respective exonic sequences, according to the Irxs genomic sequences retrieved from the published ENSEMBL's chick genome (www.ensembl.org).The PCR conditions were as follows: 10 min at 95°C, then 10 cycles (30 s at 94°C, plus 2 min at 68°C, and 2 min at 72°C), followed by 20 cycles (30 s at 94°C, plus 2 min at 68°C to 58°C – down 0.5°C per cycle – and 2 min at 72°C), and, at the end, 10 cycles (30 s at 94°C, plus 2 min at 55°C, and 2 min at 72°C). The last step of PCR conditions was 10 min at 72°C. The PCR products were cloned into pGEM-T Easy Vector (Promega) and sequenced (SAI, University of Murcia).

In situ hybridization staining procedure

In situ hybridization was performed on cryosections as described by Sánchez-Guardado et al. (2009, 2011, 2013). Plasmid information is provided in Table 1. The *Fgf10* probes were the same as used previously (Sánchez-Guardado et al. 2013). All riboprobes were labeled with digoxigenin-11-UTP (Roche, Mannheim, Germany) according to the manufacturer's instructions. *In situ* hybridization was performed on cryosections following the methods described by Sánchez-Guardado et al. (2009, 2013). The sections were post-fixed with 4% paraformaldehyde in PBS for 10 min, rinsed with PBS for 15 min, then acetylated in a solution containing 234 ml of distilled water, 3.2 ml of triethanolamine (Sigma), 420 ml of 36% HCl, and 600 ml of acetic anhydride. After acetylation, the sections were permeabilized in 1% Triton X-100 for 30 min, and then pre-hybridized at room temperature for 2 h in a solution containing 50% formamide, 10% dextran sulfate (Sigma), 5× Denhardt's solution (Sigma), and 250 mg/ml tRNA (Roche), in salt solution. Hybridization was performed with 200-300 ng/ml of the probe in the same hybridization solution overnight at 72°C. After hybridization, the sections were rinsed with 0.2% SSC at 72°C for 1-2 h, and then twice with a solution containing 100 mM NaCl and 100 mM Tris-HCl (pH 7.5). After treatment with 10% normal goat serum (NGS) in the same solution for 2 h, the sections were incubated overnight with alkaline phosphatase-conjugated anti-digoxigenin Fab fragments (Roche, 1:3500). The sections were rinsed twice with the same buffer, and then incubated in 100 mM NaCl, 50 mM $MgCl_2$, and 100 mM Tris-HCl (pH 9.5). The colouring reaction was developed with NBT and BCIP (Roche). The sections were rinsed with PBS and coverslipped with Mowiol (Calbiochem, Bad Soden, Germany). No signal was obtained with the sense probes. For more details about the *in situ* hybridization procedure, see Ferran et al. (2015).

Immunohistochemistry staining procedure

Immunohistochemistry with 3A10 antibody (1:40; Antibody ID from NIF: AB_531874; Developmental Studies Hybridoma Bank (DSHB), mouse, monoclonal, #3A10; Sánchez-Guardado et al. 2013) was also performed on cryosections as previously described by Sánchez-Guardado et al. (2009, 2011, 2013). The primary antibody was reacted with biotinylated goat anti-mouse secondary antibody (1:100; Sigma), and then with ExtrAvidin-biotin-horseradish peroxidase complex (1:200; Sigma). All antibodies were diluted in a solution containing 1% NGS and 0.25% Triton X-100 in PBS. The histochemical detection of the peroxidase activity was carried out by using 0.03% diaminobenzidine (DAB) and 0.005% H_2O_2. After the immunoreactions, the sections were rinsed three times with PBS-T and then coverslipped with Mowiol.

Imaging

All preparations were photographed with a Zeiss Axiophot microscope equipped with a Zeiss AxioCam camera (Carl Zeiss, Oberkochen, Germany) and AxioVision 2.0.5.3. software, and the images were saved in 4-MB TIFF format. These were size-adjusted, cropped, contrast enhanced, and annotated with Adobe Photoshop version 7.0 software (Adobe Systems, San Jose, CA). All illustrations were produced with this Adobe Photoshop software.

RESULTS

Cluster A and cluster B expression patterns at the otic vesicle stage (HH18)

At stage HH18, the expression patterns of *Irx* genes belonging to cluster A (*Irx1*, *Irx2*, and *Irx4*) or cluster B (*Irx3*, *Irx5*, and *Irx6*) showed great similarity. For this reason, the expression pattern of one representative member of each cluster will be described: *Irx1* for cluster A and *Irx3* for cluster B. In contrast, *Irx4* signal was not detected in the developing otic epithelium from stage HH18 to HH27 (not shown).

At the otic vesicle stage (HH18), the *Fgf10*-expressing domain, found in the ventromedial portion of the otic epithelium, corresponds to a large prosensory domain from which almost all sensory elements will arise (Fig. 1c; Sánchez-Guardado et al. 2013). For this reason, the expression patterns of *Irx1*, *Irx3*, and *Fgf10* genes will be compared with each other in serial horizontal sections through the otic vesicle (ov; Fig. 1a-c). *Irx1* transcripts (representing cluster A genes) were observed mostly in the vesicle's lateral wall, forming an anteroposterior band (Fig. 1a). High levels of *Irx1* expression were detected in the anterior and posterior poles of the otic anlage (long arrows in Fig. 1a), whereas less *Irx1* expression was observed at its lateral wall (short arrow in Fig. 1a). In the anterior and posterior poles of the otic vesicle, the *Fgf10*-labeled presumptive territories of the anterior and posterior ampullary cristae were *Irx1*-positive (ac and pc; Fig. 1a, c; see also Sánchez-Guardado et al. 2013). Concerning the *Irx3* gene (representing cluster B genes), its expression was observed mainly in the posterior portion of the otic vesicle (long arrow in Fig. 1b), including the presumptive territory of the posterior ampullary crista, *Fgf10*-positive (pc; Fig. 1b, c). In this area, the posterior part of the strongly *Irx1*-labeled domain overlapped with the posterior *Irx3*-expressing area (Fig. 1a, b). However, the *Irx3*-stained area extended medially more than the *Irx1*-expressing area did (Fig. 1a, b). *Irx3* expression was also detected in the anterolateral wall of the otic vesicle (short arrow in Fig. 1b), in an area delimiting the presumptive territory of the *Irx1*-positive anterior ampullary crista (ac; see arrowheads in Fig. 1a-c). We cannot exclude a very low expression of *Irx3* gene in the lateral wall of the otic epithelium (black asterisk in Fig. 1b). Regarding the presumptive territory of the developing endolymphatic apparatus, the members of cluster B were the only *Irx* genes expressed in it (Fig. 1b'; not shown for cluster A). Figures 1d-g summarize these results.

At the vesicle stage (HH18), a strong *Irx1* expression was observed in the acoustic-vestibular ganglion (AVG) (white asterisk in Fig. 1a), but this showed weak *Irx3* expression (white asterisk in Fig. 1b).

Cluster A and cluster B expression patterns at stages HH24/25

At stage HH24/25, the inner ear shows significant morphogenetic changes. The presumptive territories of almost all sensory patches are clearly identified on sections treated with *Fgf10* probes (Fig. 2d, g, j, m; Sánchez-Guardado et al. 2013). Horizontal sections through the dorsal aspect of the stage HH24/25 otic anlage showed strong *Irx1* expression patches (cluster A) in its anterior and posterior poles, particularly in the latter (Fig. 2a). A strong *Irx1* expression labeled also a small area in the anterolateral wall (black asterisk in Fig. 2a) which delimited laterally the *Fgf10*-positive anterior crista (ac in Fig. 2a, d). This strongly *Irx1*-stained portion of the otic epithelium corresponds to a part of the anterior vertical pouch (a-vp; Fig. 2a). Interestingly, the developing anterior crista itself showed weaker expression of the *Irx1* gene (ac; between rostral arrowheads in Fig. 2a, d). In the posterior region of the same section, heterogeneous levels of *Irx1* expression were detected in the developing posterior vertical pouch (p-vp and arrows in Fig. 2a). The presumptive domain of the *Fgf10*-positive posterior crista (pc; between posterior arrowheads in Fig. 2a, c) was also clearly labeled by the *Irx1* expression (pc in Fig. 2a). A significant diminution of *Irx1* expression was now detected in the lateral wall (short arrow in Fig. 2a; see also short arrows in Fig. 2e, h). Part of the opposite medial wall was completely devoid of *Irx1* expression (Fig. 2a; see also Fig 2e, h). The endolymphatic system was also devoid of *Irx1* transcripts (not shown).

In adjacent ventral sections (Fig. 2e-j), strong *Irx1* expression was observed in the dorsolateral part of the *Fgf10*-positive macula utriculi (mu; Fig. 2e, g), but not in its ventral part (mu; Fig. 2h, j). A weaker expression of *Irx1* in the lateral crista is noteworthy (lc in Fig. 2e); this starts to be marked by weak *Fgf10* expression at this developmental stage, HH24/25 (lc in Fig. 2g; Sánchez-Guardado et al. 2013). The *Fgf10*-labeled macula sacculi did not display any expression of *Irx1* (ms in Fig. 2h, j). At this level, the posterior heterogeneous *Irx1*-labeling domains (arrows in Fig. 2e, h) included the posterior crista (pc; Fig. 2e, g) and the macula neglecta (mn; Fig. 2h, j). The presumptive territory of the posterior crista showed, therefore, different levels of *Irx1* expression, which were more intense ventrally than dorsally (pc; compare Fig. 2a and Fig. 2e).

The *Irx1*-expressing domain observed in the posterior pole of the otic epithelium extended ventrally in the posterior and medial walls of the cochlear duct (cd; arrows in Fig. 2k). The presumptive territory of the *Fgf10*-labeled basilar papilla (bp in Fig. 2k, m) and probably also that of the developing macula lagena (not identified at this developmental stage by means of specific markers; Sánchez-Guardado et al. 2013) were included within this *Irx1*-expressing domain. Figures 3a and b summarize the *Irx1* expression pattern in the otic epithelium at stages HH24/25.

In the stage HH24/25 inner ear, a very weak *Irx3* expression (cluster B) was observed in the endolymphatic duct (ed; Fig. 2c). In the vestibule, a very weak *Irx3* expression was also detected in a small rostral portion of the lateral wall, just at the level of the developing *Fgf10*-positive lateral crista (lc in Fig. 2f, g). A very small portion of the *Fgf10*-stained utricle macula showed a very low level of *Irx3* expression just adjacent to the lateral crista (mu in Fig. 2f, g). However, the macula sacculi was entirely *Irx3* negative (Fig. 2f, i). Strong *Irx3* expression patches were observed in the medial wall of the otic anlage (long arrows in Fig. 2b, f, i). In contrast, very low levels of *Irx3* expression, almost undetectable, were observed in its posterior and lateral walls (short arrows in Fig. 2b, f, i). The *Fgf10*-positive posterior crista (Fig. 2d, g) was included within this weakly *Irx3*-expressing domain (pc; Fig. 2b, f). In adjacent ventral sections (Fig. 2i, j), the weakly *Fgf10*-staining macula neglecta was clearly *Irx3* positive (mn in Fig. 2i, j). In the developing cochlear duct, a heterogeneous *Irx3*-expressing area was observed in almost its entire wall (short arrows in Fig. 2l). In horizontal sections across it, a portion of the *Fgf10*-positive basilar papilla was labeled by *Irx3* expression (bp in Fig. 2l, m). Figures 3c and d summarize the *Irx3* expression pattern in the otic epithelium at stages HH24/25.

The acoustic-vestibular ganglion also showed expression of both genes, though the signal was much stronger for *Irx1* (AVG; white asterisks in Fig. 2a, e, h) than for *Irx3* (black asterisks in Fig. 2f, i).

Cluster A and cluster B expression patterns at stage HH27

At stage HH27, the morphogenetic changes are more evident and all the sensory epithelia are easily recognized by their *Fgf10* expression (Sánchez-Guardado et al. 2013). Horizontal sections through the dorsalmost portion of the stage HH27 inner ear show weak *Irx1* expression (cluster A) in its anterior aspect. A very small portion of the proximal endolymphatic duct presented now *Irx1* expression (not shown; see Fig. 5a, b),

in contrast with earlier stages (Figs. 2 and 3). At this developmental stage, the *Fgf10*-positive anterior crista showed a more evident *Irx1* expression (ac; Fig. 4a, c) than at a previous stage (HH24, Fig. 2a, d). In the posterior portion of the inner ear, *Irx1* expression was observed in the developing posterior vertical pouch (p-vp and long arrow in Fig. 4a), including the strongly *Fgf10*-labeled posterior crista (pc; Fig. 4a, c) and the weakly *Fgf10*-defined macula neglecta (mn; Fig. 4a, c). In horizontal sections through the central part of the vestibule (Fig. 4d-f), the *Fgf10*-positive lateral crista and most of the developing horizontal pouch wall showed weak *Irx1* expression (lc and hp; Fig. 4d, f). In the utricle and saccule (u and s; Fig. 4d), very low *Irx* expression was detected in their posterior walls (short arrows in Fig. 4d), while the *Fgf10*-expressing utricular and saccular maculae were *Irx1* negative (mu and ms; Fig. 4d, f). In the posterior aspect of the stage HH27 inner ear, a very heterogeneous *Irx1* expression was observed in the area of the otic epithelium in which the cochlear duct opens into the vestibule (cd in Fig. 4d). *Irx1* expression was very strong in its lateral aspect (long arrow in Fig. 4d), whereas very weak *Irx1* signal was seen in its medial wall (black asterisk in Fig. 4d). These *Irx1* positive areas extended ventrally in the well-defined cochlear duct (cd; Fig. 4g, j). A stronger labeling was restricted to its caudolateral wall (long arrow in Fig. 4g), whereas weak reaction occupied a larger area (short arrows in Fig. 4g, j). The *Fgf10*-positive basilar papilla and macula lagena were included within this weakly *Irx1*-expressing domain (bp and ml; Fig. 4g, i, j, l). Figures 5a and b summarize the *Irx1* expression pattern in the otic epithelium at stage HH27.

Concerning the *Irx3* gene (cluster B), the endolymphatic apparatus distinctly showed *Irx3* expression at stage HH27 (not shown; see Fig. 5c, d). Horizontal sections through the vestibule (Fig. 4b, e) showed that at stage HH27, but not before (compare stage HH24; Fig. 2b), the *Fgf10*-positive anterior crista presented a perceptible amount of *Irx3* transcripts (ac; Fig. 4b, c). The most evident *Irx3* expression was observed at the posterior otic epithelium (arrows in Fig. 4b, e), including a large portion of the developing posterior vertical pouch (p-vp; Fig. 4b), the posterior crista (pc; Fig. 4b), and the macula neglecta (mn; Fig. 4b). The lateral crista and a portion of the adjacent developing horizontal pouch showed weak *Irx3* expression (lc; Fig. 4e). The utricular and saccular maculae were devoid of any *Irx3* transcripts (mu and ms; Fig. 4e). Similarly as with the *Irx1* gene, very low *Irx3* expression was detected in the posterior walls of the utricle and saccule (u and s; short arrows in Fig. 4e). In the posterior aspect of the otic anlage, *Irx3* expression was evident in the most proximal part of the cochlear duct (long arrow and cd in Fig. 4e), contiguously to the saccule (s in Fig. 4e). In the

cochlear duct (cd; Fig. 4h, k), variable *Irx3* expression occupied almost all its wall (cd; short arrows in Fig. 4h, k), including the *Fgf10*-positive basilar papilla (bp; Fig. 4h, i) and the *Fgf10*-positive macula lagena (ml; Fig. 4k, l). At this level, the extent of *Irx1* and *Irx3* expression was very similar (Fig. 4g, h). Figures 5c and d summarize the *Irx3* expression pattern in the otic epithelium at stage HH27.

The mesenchyme surrounding the otic epithelium also showed high levels of *Irx3* transcripts (asterisks in Fig. 4b). In previous descriptive studies, the expression of four *Irx* genes (*Irx1*, *Irx2*, *Irx3*, and *Irx5*) was also detected in the underlying mesenchyme, but *Irx4* and *Irx6* were absent (Bosse et al. 1997; Houweling et al. 2001; Mummenhoff et al. 2001; for the *Iroquois-related homeobox like-1* (*Irxl1*) gene, see Liu et al. 2006). As occurred at previous stages, the acoustic-vestibular ganglion displayed strong *Irx1* expression (AVG; white asterisk in Fig. 4g) and weaker *Irx3* expression (white asterisk in Fig. 4e).

Expression pattern of cluster A at stage HH34

At 8th days of incubation (stage HH34), all the innervated and *Fgf10* positive sensory elements, as well as the non-sensory elements of the inner ear are clearly defined (Sánchez-Guardado et al. 2013). In horizontal sections through the inner ear vestibule, it could be clearly seen that the members of the IrxA cluster (*Irx1*, *Irx2*, and *Irx4*) showed different expression patterns (Figs. 6, 7, and 8). Regarding the *Irx1* gene, the lateral wall of the common crus (cc in Fig. 7) showed strong *Irx1* expression (short arrow in Fig. 6a). The endolymphatic apparatus wall was *Irx1* negative (ed in Fig. 6a). Heterogeneous/variable expression was observed in the developing semicircular canals (long arrows in Fig. 6a, a', c). No *Irx1* expression was detected in the cristae (ac and pc, Fig. 6a, a'; lc, Fig. 6c). However, the macula neglecta clearly showed *Irx1* expression (mn; Fig. 6a). Ventrally, a small portion of the utricle (u) also showed *Irx1* transcripts (short arrow in Fig. 6c). The utricular and saccular maculae did not display any *Irx1* expression (mu and ms in Fig. 6c). In the cochlear duct (Fig. 6c, e, f), a dorsoventrally arranged, narrow band expressing *Irx1* was detected in its posterolateral wall (asterisk in Fig. 6c and short arrows in Fig. 6e, f), including the posterior part of the developing tegmentum vasculosum (tv in Fig. 6e, f). The basilar papilla and the macula lagena were *Irx1* positive (bp and ml in Fig. 6e, f). The vestibular ganglion (VG; Fig. 6c') and the acoustic ganglion (AG, and asterisk in Fig. 6e) showed *Irx1* signal.

Regarding the *Irx2* gene, it is noteworthy that its expression pattern is different from

that of *Irx1*. *Irx2* expression was detected in all sensory patches (cristae, maculae, and basilar papilla; between arrowheads in Fig. 6b, d, g, h), which showed high levels of *Irx2* transcripts at this developmental stage. In the case of non-sensory elements, the lateral wall of the common crus (cc in Fig. 7) showed strong *Irx2* expression (short arrow in Fig. 6b). A portion of the epithelium of the posterior ampulla, adjacent to the *Irx2*-positive macula neglecta (mn; Fig. 6b), was also labeled by the *Irx2* probe (long arrow in Fig. 6b). The endolymphatic apparatus wall was *Irx2* negative (ed in Fig. 6b). *Irx2* expression was clearly detected in the posterolateral wall of the developing cochlear duct (asterisk in Fig. 6d and short arrows in Fig. 6g, h), similarly to *Irx1* expression (Fig. 6c, e, f). The tegmentum vasculosum develops within this cochlear *Irx2*-expressing area (short arrows and tv in Fig. 6g, h). The vestibular ganglion (VG; Fig. 6d') and the acoustic ganglion (AG and asterisk in Fig. 6g) clearly showed *Irx2* expression. Figure 7 summarizes the expression patterns of the *Irx1* and *Irx2* genes in the otic epithelium at stage HH34.

Expression of *Irx4*, the third component of the IrxA cluster, was not observed at earlier developmental stages. At stage HH34, *Irx4* transcripts appeared in scattered cells of the utricular and saccular maculae (mu and ms; short arrows in Fig. 8a; see short arrow in Fig. 8a' for the mu). *Irx4*-stained cells were not detected in the cristae (see lc in Fig. 8a; not shown for ac and pc). More evident *Irx4* expression appeared in the lateral wall of the region between the saccular cavity and the cochlear duct (s and cd; long arrow in Fig. 8a). This *Irx4* expression extended ventrally into the cochlear duct wall (long arrows in Fig. 8b, c), including the anterior part of the tegmentum vasculosum (tv; arrow in Fig. 8b). *Irx4* expression was also observed in the most anterior half of the basilar papilla (bp in Fig. 8b), similarly as with *Irx1* expression (Fig. 6e). In the anterior aspect of the cochlear duct, a clearcut gap of *Irx4* expression was observed in a small area corresponding to the *Fgf10*-positive non-sensory area contiguous to the innervated basilar papilla (short arrow in Fig. 8b; see Sánchez-Guardado et al. 2013). The macula lagena at the end of the cochlear duct (ml in Fig. 8c) and the macula neglecta in the vestibule (not shown) did not display *Irx4* expression. There was no *Irx4* expression in the acoustic and vestibular ganglia (AG; Fig. 8b; VG, not shown). Figures 8d and e summarize the *Irx4* expression patterns in the otic epithelium at stage HH34.

Expression pattern of cluster B at stage HH34

At stage HH34, the expression patterns of the different *Irx* genes belonging to the IrxB cluster (*Irx3*, *Irx5*, and *Irx6*) were dissimilar (Figs. 9 and 10); those of *Irx3* and *Irx6*

were more closely related (Fig. 9). We shall describe mainly the *Irx3* expression pattern (Fig. 9), indicating some differences in the *Irx6* pattern (Fig. 9b'). At this developmental stage, the endolymphatic apparatus showed expression of both *Irx3* and *Irx6* genes this being more evident for the endolymphatic duct (ed in Fig. 9a) than for the endolymphatic sac (es; not shown). A small portion of the common crus wall displayed clear *Irx3*/*Irx6* expression (short arrows in Fig. 9a). *Irx3* and *Irx6* transcripts were also detected in portions of the ampullae, though the sensory elements were negative for both genes (ac, pc, and lc; long arrows in Fig. 9a, b). The macula neglecta was *Irx3* and *Irx6* positive (mn in Fig. 9a). In the utricular and saccular compartments, *Irx3* expression was observed in the macula utriculi (mu in Fig. 9b), but not in the macula sacculi (ms in Fig. 9b). However, *Irx6* transcripts were present in both sensory elements (mu and ms in Fig. 9b'). This was the only dissimilarity observed between *Irx3* and *Irx6* genes in the membranous labyrinth. In the most proximal portion of the cochlear duct, strong expression of *Irx3* and *Irx6* was readily detectable (short arrows in Fig. 9b), next to the saccule (s; Fig. 9b). The rest of the cochlear duct showed heterogeneous expression of both genes (short arrows in Fig. 9c, d). The basilar papilla and the macula lagena were excluded from the *Irx3*/*Irx6*-expressing domain (bp and ml in Fig. 9c, d). Expression of *Irx3* and *Irx6* bordered some parts of the basilar papilla and the entire macula lagena (Fig. 9c, d). The vestibular ganglia showed *Irx3* expression (not shown), whereas the acoustic ganglion was weakly *Irx3* positive (AG and black asterisk in Fig. 9c). Both ganglia were devoid of *Irx6* expression (not shown). Figures 9e and f summarize the *Irx3* expression pattern in the otic epithelium at stage HH34.

Irx5 expression was observed in a small portion of the endolymphatic apparatus (not shown) and in the cochlear duct (cd; arrows in Fig. 10a-d). The ventral aspect of the macula sacculi was delimited by *Irx5* expression (arrowhead in Fig. 10b), but not so its dorsal aspect (arrowhead in Fig. 10a). This *Irx5*-expressing domain extended ventrally into the posterior wall of the cochlear duct (arrows in Fig. 10b, c), delimiting medially the developing tegmentum vasculosum (tv; Fig 10c). *Irx5* expression was absent in all sensory patches (ms and mu, Fig. 10a, b; bp in Fig. 10c, d; ml in Fig. 10d; cristae and mn, not shown). The neurons of the vestibular and acoustic ganglia did not show any expression of *Irx5* (AG in Fig. 10c; VG, not shown). Figures 10e and 11f summarize the *Irx5* expression pattern in the otic epithelium at stage HH34.

DISCUSSION

During inner ear development, intricate networks of signaling pathways promote patterning of the early otic primordia, establishing compartments of restricted cell lineages and consequent cell fate specification. These developmental mechanisms are mediated directly by asymmetrical expression of given regulator genes and local cell-cell interactions (Fekete 1996; Brigande et al. 2000; Fekete and Wu 2002; Sánchez-Guardado et al. 2014). It is interesting that dynamic expression of *Irx* genes could have a key role for tissue specification (and probably also for morphogenesis) during development in many phyla, controlling genetic pathways involved in boundary generation (Cavodeassi et al. 2001; Gómez-Skarmeta and Modolell 2002). In *Drosophila*, iroquois complex (*iro-C*) expression in the dorsal aspect of the eye disk, acting as a compartment selector mechanism, mediates emergence of a dorsoventral eye organizer and corresponding cell lineage restrictions (McNeil et al. 1997; Dominguez and Celis 1998; Papayannopoulos et al. 1998; Cavodeassi et al. 1999; Yang et al. 1999; Pichaud and Casares 2000). Interestingly, *Hh* expression is induced at the interface between the *Irx*-expressing and *Irx*-non-expressing domains (Cavodeassi et al. 1999). Also, the *Drosophila* BMP2/4 homologue Dpp represses *Iro-C* in the most proximal part of the notum, regulating its subsequent subdivision into medial and lateral parts (Cavodeassi et al. 2002). In addition, *Iroquois* genes in *Drosophila* may act as transcriptional activators of proneural genes (Gómez-Skarmeta et al. 1998; Gómez-Skarmeta and Modolell 2002). Therefore, the *Irx* genetic family also may be directly involved in axial specification and patterning of the developing otic epithelium.

Irx genes in the early patterning stages of developing epithelia

Irx genes are directly involved in the specification of the pre-placodal field and its placodal derivates (Itoh et al. 2002; Glavic et al. 2004; Schlosser and Ahrens 2004; Lecaudey et al. 2005; Rodríguez-Seguel et al. 2009; see Schlosser 2005, 2006). As development proceeds, at least eight of eleven *Iro* genes studied in zebrafish participate in the formation of derivates from the posterior placodal field (Itoh et al. 2002; Lecaudey et al. 2005; Feijóo et al. 2009). In *Xenopus*, *Irx2* expression in placodes also confirms the involvement of *Irx* genes in placodal specification (Rodríguez-Seguel et al. 2009). In the chick, *Irx1* and *Irx2* genes, members of the IrxA cluster, show a similar expression pattern. Both genes are expressed in almost the entire extent of the otic placode and cup (stage HH11-12), except in a small domain located at their most anterior portion, whereas *Irx4* signal is completely absent (Geisha database). In the early

chick otic cup, the anterior proneural domain is defined by the expression of *Sox3* and *Fgf10* genes, whereas the complementary posterior non-neural domain is characterized by the expression of *Irx1* and *Lmx1b* genes. The *Notch* signaling pathway seems to be required for maintaining proneural and non-neural identities in this early pattern without any cell mixing between the two compartments (Abelló et al. 2007). Therefore, *Irx* genes participate in the accurate development of anteroposterior compartments of the cephalic ectoderm.

The molecular mechanisms involved in early anteroposterior patterning of the otic placode, which are directly triggered by signals emanating from adjacent tissues, need to be better understood (Groves and Fekete 2012; Bok et al. 2007a, 2011; Hammond and Whitfield 2011). In zebrafish embryos, FGF and SHH activities may represent independent, instructive antagonists in pre-patterning of the otic placode, conferring asymmetric anterior *versus* posterior identities, respectively (Hammond and Whitfield 2011). In the inner ear of amniotes, retinoic acid (RA) also promotes posterior identity in both mouse and chick, probably regulating the expression of *Tbx1*, a posterior otic marker (Bok et al. 2011). At present, it remains unclear how to bring together the dissimilar anteroposterior patterning models proposed in anamniote and amniote vertebrates in both functional and evolutionary contexts (Groves and Fekete 2012), discerning how *Irx* genes might participate in these patterning events.

Irx genes in the specification of the rostrocaudal and dorsoventral axes

In the developing neural tube of vertebrates, restricted *Irx* expression patterns define differential molecular identities establishing boundaries along the rostrocaudal and dorsoventral axes (Bosse et al. 1997, 2000; Casarosa et al. 1997; Bellefroid et al. 1998; Gómez-Skarmeta et al. 1998; Goriely et al. 1999; Tan et al. 1999; Briscoe et al. 2000, 2001; Novitch et al. 2001; Cohen et al. 2000; Peters et al. 2000; Sato et al. 2001; Glavic et al. 2002; Itoh et al. 2002; Kobayashi et al. 2002; Lecaudey et al. 2004, 2005; Matsumoto et al. 2004; Hirata et al. 2006; García-Campmany and Martí 2007; Rodríguez-Seguel et al. 2009; Pose-Méndez et al. 2015). The *Irx* gene family be directly involved in patterning of the developing membranous labyrinth once the otic vesicle is formed. In *Xenopus*, the expression of *Irx1-5* genes is observed in the otic vesicle at the tail bud stage, more evidently in its posterior aspect (Rodríguez-Seguel et al. 2009). In the mammalian otic vesicle, *Irx1* expression labels a part of the otic lateral wall, whereas *Irx2* expression appears at the ventrolateral wall, with some overlap of the two genes (Bosse et al. 1997). In contrast, mouse *Irx3* expression is restricted to the

ventromedial portion of the otic vesicle, in an area adjacent to the hindbrain (Bosse et al. 1997). *Irx5* expression seems to overlap such *Irx3* expression (Bosse et al. 2000; Houweling et al. 2001). Interestingly, whole-mount *in situ* hybridization shows that *Irx1* and *Irx2* expression is clearly restricted to the posterior part of the mouse otic vesicle (Bosse et al. 1997); this suggests the implication of *Irx* genes in the specification of the rostrocaudal (anteroposterior) axis of the otic anlage. Therefore, *Irx* genes may directly govern pattern formation during the development of amphibian and mammalian inner ears, at least at the otic vesicle stage (Bosse et al. 1997; Goriely et al. 1999; Mummenhoff et al. 2001; Rodríguez-Seguel et al. 2009).

Few studies examining *Irx* genes in the avian otocyst have been reported . At a late otic vesicle stage, HH20, our detailed study of serial cryostat sections showed clearcut expression of *Irx1* and *Irx2* genes (cluster A) in an anteroposterior band located in the lateral wall of the otocyst (present results; see Goriely et al. 1999 for *Irx2* at stage HH15-16). These expressions overlapped rostrally and caudally the *Fgf10*-positive domain, consequently including the presumptive territories of the anterior and posterior cristae. The expression of Irx cluster B genes, represented here by *Irx3*, was observed mostly at the posterior wall of the otic vesicle, but also in its lateral wall. *IrxB* expression overlapped the *Fgf10*-expressing domain caudally, but not rostrally, thus delimiting the presumptive domain of the anterior crista. The presumptive territory of the endolymphatic apparatus was also included in the cluster-B-positive domain (present results). Accordingly, the B cluster may govern the specification of a larger area than cluster A. *Irx* genes seem therefore directly involved in axial patterning of the otic anlagen, contributing in particular to the early specification of the lateral and posterior aspects of the otic vesicle.

The WNT signaling pathway operating from the dorsal aspect of the neural tube seems required for the specification of the dorsal aspect of the otic anlagen; WNT factors regulate the expression of such dorsal otic genes as *Dlx5, Dlx6,* and *Gbx2* (Riccomagno et al. 2005). In addition, BMP diffusing from the dorsal neural tube may also participate in the regionalization of the otic placode (Abelló et al. 2010). It is well known that these diffusible signals (WNT and BMP) also can regulate *Irx* functions during embryonic epithelial patterning (Briscoe et al. 2000, 2001; Gómez-Skarmeta et al. 2001; Gómez-Skarmeta and Modolell 2002; Itoh et al. 2002). During neural plate specification, the mutual repression of *Xiro1/2* and *Bmp4* seems also to be modulated by the WNT signaling pathway (Gómez-Skarmeta et al. 2001; Gómez-Skarmeta and Modolell 2002),

suggesting that WNT and BMP signals may play antagonistic roles (Kudoh and Dawid 2001). On the other hand, SHH secreted from the floor plate and notochord is required for the ventral specification of the otic anlagen (Liu et al. 2002; Riccomagno et al. 2002, 2005; Bok et al. 2005; for review, see Bok et al. 2007a); this involves gradients of repressor and activator forms of *Gli* in a dose-dependent manner (Bok et al. 2007b). Interestingly, the SHH signal also controls dorsoventral patterning of the developing spinal cord, regulating among other signals *Irx* expression (Bosse et al. 1997; Briscoe et al. 2000, 2001). We should recall that *Gli1*, *Gli2*, and *Gli3* have been postulated as candidate regulators of *Irx* genes during mouse development (Gómez-Skarmeta et al. 1998; Zülch et al. 2001; Becker et al. 2001). Further studies will be necessary to determine the possibly pivotal role of *Irx* genes in the specification of the dorsoventral axis of the inner ear.

Irx genes may also collaborate with some selector transcription factors in the axial specification of the developing inner ear of vertebrates. *Gbx2* and *Otx2* genes are involved in dorsoventral patterning of the otic anlagen. *Gbx2* expression appears in the dorsomedial wall of the chick inner ear (Sánchez-Calderón et al. 2002, 2004), this pattern being regarded as a downstream target of the 'hindbrain-to-ear' signals (Lin et al. 2005). *Otx2* expression is observed in the ventrolateral otic wall (Sánchez-Calderón et al. 2002, 2004). The expression patterns of *Otx2* and *Gbx2* fit well with the phenotype reported in mouse mutants for these two genes (Wassarman et al. 1997; Cantos et al. 2000; Lin et al. 2005; reviewed by Bok et al. 2007a; Chatterjee et al. 2010). Interestingly, *Gbx2*, *Otx2*, and *Irx* genes are expressed in the midbrain/hindbrain organizer, where they are regarded as key factors for the specification of the meso-isthmo-cerebellar region (Bosse et al. 1997, 2000; Bellefroid et al. 1998; Gómez-Skarmeta et al. 1998; Goriely et al. 1999; Tan et al. 1999; Cohen et al. 2000; Peters et al. 2000; Sato et al. 2001; Glavic et al. 2002; Itoh et al. 2002; Hidalgo-Sánchez et al. 2000, 2005a, b; Pose-Méndez et al. 2015). In this developmental context, *Irx* genes apparently govern the extent of the *Gbx2*-expressing and *Otx2*-expressing domains in the developing otic epithelium. In *Xenopus*, the genes *Xiro1*, *Gbx2*, and *Otx2* collaborate in positioning the isthmus organizer and in the later specification of the midbrain-hindbrain domain. Thus, *Irx* genes are able to activate *Otx2* and *Gbx2* expression at different places and times (Glavic et al. 2002). Because the expression of these three transcription factors are governed by FGF and WNT morphogen signals in the specification of the midbrain-hindbrain domain (Sato et al. 2001; Hidalgo-Sánchez et al. 2005a), a similar mechanism could also be invoked in the dorsoventral or

anteroposterior patterning of the developing otic epithelium.

Irx genes may also work together with other regulatory factors during inner ear development. In *Drosophila*, *Irx-C* and muscle segment homeobox (msh) genes are expressed in adjacent domains to define the notum/dorsal hinge boundary. Loss- and gain-of-function studies have shown that *msh* represses *Irx-C* (Villa-Cuesta and Modolell 2005). In the inner ear of zebrafish embryos, *msh-d* is expressed at the dorsal aspect of the vesicle (Ekker et al. 1992). Expression of the chick *Msx-1* gene, a *msh* paralogue , is likewise detected in the dorsal portion of the avian otic vesicle (Wu and Oh 1996). Because of the expression of chick *IrxB* in the developing endolymphatic system (present data), we cannot rule out a possible cooperation of *Msx* and *Irx* genes in the specification of the developing membranous labyrinth. Also, *Six3* and *Irx3* are known to mutually regulate their expression during anteroposterior specification of the diencephalon in a context where cross-activity of FGF8, SHH, and WNT signaling pathways takes place (Kobayashi et al. 2002; Kiecker and Lumsden 2004). Since *Six1* is involved in ventral patterning of the inner ear (Zheng et al. 2003; Ozaki et al. 2004; for review, see Bok et al. 2007a), we cannot exclude an analogous molecular mechanism conserved between members of the *Irx* and *Six* families in the specification of the otic wall.

More key transcription factors might be considered. For example, *Irx7* and *Irx1b* are necessary for the correct specification of the rostral hindbrain (Lecaudey et al. 2004; Stedman et al. 2009), with *Irx7* and *Meis1.1* cooperating in the regulation of *Hoxb1a*, *Hoxa2a*, and *Krox20* expression (Stedman et al. 2009). It was reported that *Meis* genes may be involved in the specification of the dorsolateral part of the developing chick inner ear, mainly in the development of the semicircular canals and all associated cristae (Sánchez-Guardado et al. 2011). Further experiments are needed to confirm or reject these possibilities.

Irx genes in the specification of sensory elements

In the HH24/25 chick inner ear, strong expression of cluster A genes (*Irx1*) was observed in the anterior and posterior poles of the otic anlage, the posterior domain being larger than the anterior domain (present data). The expression pattern of members of cluster B genes (*Irx3*) was more restricted, being located at the posteromedial wall of the vestibule and at the posterior aspect of the cochlear duct. Therefore, *Irx* gene clusters A and B may regulate the initial specification of sensory patches in their

respective expression domain (present results). Later in development (HH34), the dynamic and heterogeneous expression pattern of *Irx* genes belonging to cluster A or cluster B, jointly with the action of other key factors, may govern the final differentiation of sensory patches.

It was reported recently that the *Fgf10* gene plays a key role in the specification of sensory epithelia in the developing chick inner ear, operating by means of two different mechanisms: (i) segregation of a broad *Fgf10*-expressing band, located in the ventromedial part of the otic vesicle, where six of eight sensory patches are generated, and (ii) *de novo* specification by later *Fgf10* -expressing patches of the lateral crista and the macula neglecta (Sánchez-Guardado et al. 2013). These functions may be subtly related to Irx gene patterns. It was concluded that Irx activity depends on a FGF8/MAP kinase network (Gómez-Skarmeta and Modolell 2002; Matsumoto et al. 2004). In the embryonic limb, *Irx2* expression appears to be inhibited by FGF8 and FGF10 (Liu et al. 2002; Díaz-Hernández et al. 2013). Also, *Irx3* is repressed by FGF4 in neural tube explants, as was confirmed by expansion of the *Irx3*-expressing domain in SU5402-treated explants (Diez-del-Corral et al. 2003). Irx functions in inner ear patterning thus may be antagonized by FGF10.

In addition, all sensory patches express the *Bmp4* gene in the developing chick inner ear (Oh et al. 1996; Wu and Oh, 1996; Sánchez-Calderón et al. 2002, 2004, 2005, 2007b; Sánchez-Guardado et al. 2009, 2011). It can be tentatively speculated that *Bmp4* and *Irx* genes influence the specification of sensory elements by mutual repression. In the specification of the neural plate, the complementary expression of *Irx2* and *Bmp4* genes at the neural/epidermal border obtaining at early developmental stages strongly suggests a mutual repression of *Irx* and *Bmp4* genes to establish contiguous restricted territories (Glavic et al. 2001; Gómez-Skarmeta and Modolell 2002). Also, *Xiro1* represses *Bmp4* in dorsal mesoderm specification in *Xenopus* (Glavic et al. 2001), *irx1a* acts as a repressor of *bmp4* in the zebrafish retina (Cheng et al. 2006), and *Zirx3* represses *Bmp4* in zebrafish organizer formation (Kudoh and Dawid 2001). Besides, in the interdigital tissue and digital primordia, TGFb inhibits the expression of *Irx1* and *Irx2* genes in a concentration-dependent manner, restricting their expression at the boundary between cartilage- and non-cartilage-forming tissue (Díaz-Hernández et al. 2013).

The correct development of the vertebrate inner ear requires RA, which probably regulates the activities of other signaling pathways in a dose-dependent manner

(Romand et al. 2006; Sánchez-Guardado et al. 2009). In the chick inner ear, RA apparently diffuses ventrally from the dorsomedial wall of the otic vesicle and regulates the specification of developing sensory patches by fixing the ultimate location of the *Raldh3*-*Gbx2*/*Bmp4*-*Fgf10* border in the vestibule at stage HH24 (Sánchez-Guardado et al. 2009). Interestingly, RA directly inhibits *Bmp4, Fgf3*, and *Fgf10* expression during inner ear development (Thompson et al. 2003; Frenz et al. 2010). It has been indicated that RA signaling may control the extent of *Irx*-expressing domains in the developing neural plate (Gómez-Skarmeta et al. 1998). In the chick otic vesicle, *Irx* genes belonging to cluster A or cluster B were absent or weakly expressed, respectively, in the presumptive territory of the *Raldh3*-positive endolymphatic apparatus (Sánchez-Guardado et al. 2009). These findings strongly suggest that RA may likewise repress IrxA and induce IrxB expression during inner ear patterning and specification. The study of teratogenic effects of RA in transcription factor expression by qRT-PCR has shown that expression of IrxA genes was reduced whereas signaling by IrxB family members was increased in response to RA (Kojima et al. 2013). In the developing chick hindlimb, RA also inhibits *Irx1* and *Irx2* expressions (cluster A) by a BMP-independent mechanism (Díaz-Hernández et al. 2013). However, *Irx3* expression is reduced in the neural tube in vitamin-A-deficient (VAD) quail (Diez-del-Corral et al. 2003). Therefore, further studies are recommended to better understand the mutual interactions of long-range diffusible BMP, FGF, and RA signals in determining the possible role of *Irx* family members in the specification of otic sensory epithelial patches in specific spatial positions.

Irx genes in the specification of hair cells

Irx genes are directly implicated in cell differentiation (Briscoe et al. 2000; Itoh et al. 2002; Lecaudey et al. 2004; Cheng et al. 2007). They are expressed in the developing mouse retina (Cohen et al. 2000; Bosse et al. 2000; Houweling et al. 2001), with *Irx5* being directly implicated in bipolar cell differentiation (Cheng et al. 2005) and *Irx1a* seeming to be required for the correct functioning of SHH signals during retinal neurogenesis (Cheng et al. 2006). Our descriptive results in the developing chick inner ear suggest that some *Irx* genes may influence cell specification in the sensory elements once these are completely differentiated at stage HH34 (E8). *Irx2* expression was clearly observed in all *Fgf10*-positive sensory elements at this developmental stage. The utricular macula was *Irx3/6* positive. *Irx6* expression also labeled the posterior portion of the saccular macula. *Irx1* expression appeared at the basilar papilla and the lagenar

macula. Also, scattered cells expressed *Irx4* in the utricular and saccular maculae and in the basilar papilla. In the chick, *Cath1* is characteristically expressed by hair cells in every sensory element of the inner ear (see Sánchez-Guardado et al. 2013). These findings and the co-expression of *Irx1* and *Mash1*/*Cath1* genes in different regions of the developing nervous system (midbrain, hindbrain, and spinal cord), associated with emergence of early primary neurons, strongly suggests that *Mash1*/*Cath1* might be possible targets for *Irx* genes (present results; see also Bosse et al. 1997).

Irx genes in the specification of otic neuroblasts

It has been suggested that specification of neural fate in the *Xenopus* neural plate, may be mediated by *Irx* genes acting by means of the regulation of *neurogenin*, a proneural marker (Bellefroid et al. 1998; Gómez-Skarmeta et al. 1998). Later in development, *Irx* genes are temporarily activated in various cranial ganglia, such as the trigeminal and facial ganglia (Bosse et al. 1997). *Irx1b* and *Irx7* genes apparently play a key role in the determination of neurons in the trigeminal placode by means of the induction of ectopic *ngn1* expression (Itoh et al. 2002; Lecaudey et al. 2004). In addition, it has been indicated that *Irx3* similarly regulates *NeuroM*, which is another proneural marker (Diez-del-Corral et al. 2003). In contrast, *Xiro3* over-expression reduces the differentiation of early primary neurons, preventing the expression of such neuronal markers as N-tubulin (Bellefroid et al. 1998).

In zebrafish embryos, neuronal precursors delaminating from the otic vesicle to form the acoustic-vestibular ganglion (AVG) express the *irx1b* and *irx4b* genes (Lecaudey et al. 2005). The expression of other members of the *irx* family (*irx1a*, *irx1b*, *irx2a*, *irx5a*, and *irx5b*) has also been observed in neuroblasts within this ganglion (Lecaudey et al. 2005). In mouse embryos, strong expression of nearly all *Irx* genes is detected in the AVG at E11.5 (Bosse et al. 1997; Houweling et al. 2001), the exception being *Irx4* (Houweling et al. 2001). In the developing chick inner ear, *Irx* genes members of clusters A and B showed strong and a weak expression , respectively, in neuroblasts of the AVG from stages HH20 to HH27. At stage HH34, there was clearcut expression of *Irx1* and *Irx2* in both vestibular and auditory ganglia, and a weaker signal of *Irx3* in the vestibular ganglion. These results suggest a direct implication of *Irx* genes in otic neurogenic events (present results). Moreover, *Irx* genes may be involved in axonal pathfinding. In the chick retina, *Irx4* over-expression represses the expression of the axon guidance molecule Slit1 (Jin et al. 2003). Although *Irx4* expression was not detected in the developing chick AVG, we momentarily cannot exclude the involvement

of other *Irx* genes in otic axonal pathfinding.

ACKNOWLEDGEMENTS

This work was supported by: grant sponsor: Spanish Ministry of Science, BFU2010-19461; grant sponsor: Junta de Extremadura, GR10152 (to M.H.-S.); grant sponsor: MICINN, BFU2006-15530-C02/BFI (to L.R.-G.); grant sponsor: Spanish Ministry of Science, BFU2005-09378-C02-01; grant sponsor: MICINN, BFU2014-57516P; grant sponsor: SENECA Foundation, 19904/GERM/15 (to L.P.); grant sponsor: MICINN, BFU2006-15530-C01/BFI (to P.A); grant sponsor: Junta-de-Extremadura predoctoral fellowship, PRE/08031 (to L.-O.S.-G.). The 3A10 antibody developed by T.M. Jessell and J. Dodd was obtained from the Developmental Studies Hybridoma Bank developed under the auspices of the NICHD and maintained by The University of Iowa, Department of Biology, Iowa City, IA, USA.

CONFLICT OF INTEREST STATEMENT

The authors declare no conflict of interest.

FIGURE LEGENDS

Figure 1. Cluster A (*Irx1*) and cluster B (*Irx3*) expression patterns at the otic vesicle stage, HH18. Horizontal sections were treated with the probes indicated. Strong *Irx1* expression was detected in the anterior and posterior poles of the otic vesicle (long arrows in **a**), overlapping rostrally and caudally the *Fgf10*-positive domain (**c**; see arrowheads in **a**, **c**). The *Irx1*-expressing domain included the anterior and posterior cristae (ac and pc; **a**, **c**). A weaker *Irx1* expression was also detected in the lateral wall (short arrow in **a**). *Irx3* expression was observed mostly in the posterior otic wall (long arrow in **b**), as well as in a small territory at rostral level (short arrow in **b**). *Irx3* expression overlapped the *Fgf10*-expressing domain caudally, but not rostrally (see arrowheads in **b**, **c**), delimiting rostrally the presumptive domain of the anterior crista (ac; see arrowheads in **b**, **c**). *Irx3* expression also clearly labeled the endolymphatic apparatus (ed in **b'**) and very weakly the lateral wall (black asterisk in **b**). *Irx1* and *Irx3* genes appear expressed in the acoustic-vestibular ganglion (AVG; white asterisks in **a**, **b**). **d-g**, 3D diagrams of *Irx1*, *Irx3*, and *Fgf10* expression patterns, showing anterior (**d, f**) and posterior views (**e**, **g**) of the otic vesicle. Dotted areas represent the *Fgf10*-positive domain. For the abbreviations, see the list. Orientation: A, anterior; D, dorsal; M, medial, P, posterior. Scale bar = 130 μm in **c** (applies to **a**, **b**, **c**) and 120 μm in **b'** (applies to **b'**).

Figure 2. Cluster A (*Irx1*) and cluster B (*Irx3*) expression patterns at stage HH24/25. Horizontal sections through the inner ear anlagen, as indicated in Fig. 3, treated by *in situ* hybridization with the probes marked in each column. *Fgf10* expression was used to identify sensory patches in the developing otic epithelium (between arrowheads in **d**, **g**, **j**, **m**). In the vestibule, strong *Irx1* expression was observed in the anterolateral portion of the stage HHH24/25 inner ear (asterisk in **a**), bordering the anterior crista which showed low *Irx1* expressions (ac in **a**). In the utricular macula, the dorsal portion (mu; **e**), but not the ventral portion (mu; **h**), was *Irx1* positive. At this level, the lateral crista showed low *Irx1* expression (lc in **e**). In the posterior portions of the otic vesicle, *Irx1* expression was also clearly detected (long arrows in **a**, **e**, **h**). The posterior crista showed heterogeneous levels of *Irx1* expressions (pc in **a**, **e**). The macula neglecta was also *Irx1* positive (mn in **h**). In the cochlear duct, *Irx1* expression was detected in its posterior wall (arrows in **k**), the basilar papilla being likewise *Irx1* positive (bp in **k**). Evident *Irx3* expression was detected in the endolymphatic duct (ed; **c**), in the medial

wall of the vestibule (long arrows in **b**, **f**, **i**). Lower *Irx3* expression was also observed in the lateral crista (lc in **f**), in a portion of the utricular macula (mu in **f**), and in the posterior wall of the inner ear (short arrow in **b**, **f**, **i**); this last domain includes the macula neglecta (mn; **i**) and the basilar papilla (bp; **l**). The arrowheads point to interesting borders of expression for *Irx1*, *Irx3*, and *Fgf10* genes. The acoustic-vestibular ganglion showed *Irx1* and *Irx3* gene expression too (AVG; asterisks in **a**, **e**, **f**, **h**, **i**). For the abbreviations, see the list. Orientation: A, anterior; M, medial. Scale bar = 265 μm in **c** (applies to **c**) and 154 μm in **m** (applies to **a**, **b**, **d**-**m**).

Figure 3. 3D diagrams of *Irx1*, *Irx3*, and *Fgf10* expression patterns in both anterior (**a**, **c**) and posterior view (**b**, **d**) of the stage HH24/25 inner ear. Dotted areas show the *Fgf10*-positive sensory domain. Please note that the bars and letters refer to the panels of Figure 2**.** For other abbreviations, see the list. Orientation: A, anterior; D, dorsal; M, medial, P, posterior.

Figure 4. Cluster A (*Irx1*) and cluster B (*Irx3*) expression patterns at stage HH27. Horizontal sections through the inner ear, indicated in Fig. 5, treated by *in situ* hybridization with the probes indicated in each column. *Fgf10* expression was used to identify the developing sensory patches (between arrowheads in **c**, **f**, **i**, **l**). The *Irx1* gene was expressed in all cristae (ac in **a;** lc in **d;** pc in **a**). The macula neglecta (mn; **a**), the basilar papilla (bp; **g**), and the macula lagena (ml; **j**) showed *Irx1* transcripts as well. The rest of the maculae were devoid of *Irx1* expression (mu and ms in **d**). In the posterior aspect of the stage HH27 inner ear, an *Irx1*-expressing band oriented dorsoventrally was observed (long arrows in **a**, **d**, **g**). Weak *Irx1* expression was also observed in portions of the developing horizontal and vertical pouches (a-hp, p-vp, and hp; **a**, **d**), the utricle and saccule (u and s; short arrows in **d**), and the cochlear duct (cd; short arrows in **g**, **j**). The acoustic-vestibular ganglion showed strong *Irx1* expression (AVG; asterisk in **d**). Regarding the *Irx3* gene, its transcripts appeared in the anterior and posterior cristae (ac and pc in **b**), in the macula neglecta (mn in **b**), in the basilar papilla (bp in **h**), and in the macula lagena (ml; **k**). The utricular macula (mu in **e**) and the saccular macula (ms in **e**) were devoid of *Irx3* expression. Part of the utricular and saccular walls (short arrows in **e**) and the cochlear duct (cd; arrows in **h**, **k**) clearly displayed *Irx3* expression. A portion of the surrounding mesenchyme showed *Irx3* expression (asterisks in **b**). The acoustic-vestibular ganglion showed strong *Irx3* expression (AVG; asterisk in **e**). For the abbreviations, see the list. Orientation: A,

anterior; M, medial. Scale bar = 130 μm in **i** (applies to **a**-**i**) and 100 μm in **l** (applies to **j**-**l**).

Figure 5. 3D diagrams of *Irx1*, *Irx3,* and *Fgf10* expression patterns at stage HH27 in anterior (**a, c**) and posterior (**b**, **d**) views**.** Dotted areas show the *Fgf10* positive domains. Please note that the bars and letters refer to the panels of Figure 4**.** Orientation: A, anterior; D, dorsal; M, medial, P, posterior.

Figure 6. *Irx1* and *Irx2* expression patterns at stage HH34. Horizontal sections, indicated in Fig. 7, treated by *in situ* hybridization with the probes indicated in each column. The arrowheads point to the border of the sensory elements. *Irx1* expression was observed in the ampullar walls (long arrows in **a**, **a'**, **c**), in small patches at the utricular walls (short arrows in **c**), and in a very small portion of the common crus (short arrow in **a**). Also, the lateral wall of the cochlear duct was *Irx1* positive (black asterisk in **c** and arrows in **e**, **f**) where the tegmentum vasculosum develops (tv in **e** and **f**). The macula neglecta (mn in **a**), the basilar papilla (bp in **e**), and the lagenar macula (ml in **f**) were *Irx1* positive. Concerning the *Irx2* gene, all sensory elements showed strong *Irx2* expression (ac, pc in **b**; lc, mu, ms in **d**; mn in **b**; bp in **g**; ml in **h**). An evident *Irx2* expression was also detected in the lateral wall of the common crus (short arrow in **b**), in the posterior ampulla wall (long arrow in **b**), in the utricular wall (u; short arrow in **d**), as well as in the cochlear duct (asterisk in **d** and short arrows in **g, h**; see also tv in **g** and **h**). *Irx1* and *Irx2* transcripts were also detected in the vestibular and acoustic ganglia (VG, **c'** and **d'**; AG, asterisks in **e**, **g**). For the abbreviations, see the list. Orientation: A, anterior; M, medial. Scale bar = 180 μm in **b** (applies to **a**, **a'**, and **b**), 170 μm in **d'** (applies to **c**' and d'), 160 μm in **d** (applies to **c** and **d**), and 180 μm in **g** (applies to **e**-**h**).

Figure 7. 3D diagrams of *Irx1* and *Irx2* patterns at stage HH34, in both anterior (**a, c**) and posterior views (**b**, **d**). Dotted areas show the sensory elements. Please note that the bars and letters refer to the panels of Figure 6**.** Orientation: A, anterior; D, dorsal; M, medial, P, posterior.

Figure 8. *Irx4* expression pattern at stage HH34. Horizontal sections, indicated in **d** and **e**, treated by *in situ* hybridization with *Irx4* probe. The arrowheads point to the borders of the sensory patches. Scattered *Irx4*-expressing cells were present in the utricular and

saccular maculae (short arrows in **a**, **a**'). *Irx4* labeling was also observed in the lateral wall of the saccular-cochlear junction (long arrow in **a**) and in the cochlear duct (cd; long arrows in **b**, **c**), including the tegmentum vasculosum (tv in **b**). The anterior half of the basilar papilla was *Irx4* positive (bp; **b**). The short arrow in **b** points to the anterior gap of *Irx4* expression in the cochlear duct. **d** and **e** show 3D diagrams of the *Irx4* expression pattern at stage HH34 in anterior (**d**) and posterior (**e**) views. Hatched areas show the sensory elements. For the abbreviations, see the list. Orientation: A, anterior; D, dorsal; M, medial, P, posterior. Scale bar = 130 μm in **a** (applies to **a**), 70 μm in **a**' (applies to **a**'), 180 μm in **b** (applies to **b**) and 200 μm in **c** (applies to **c**).

Figure 9. *Irx3* and *Irx6* expression patterns at stage HH34. Horizontal sections, indicated in Fig. 10, treated by *in situ* hybridization with the probes indicated in each column and immunoreacted for 3A10. The *Irx3* and *Irx6* genes showed similar expression patterns in the ampullae (long arrows in **a**, **b**) and in the endolymphatic apparatus (ed in **a**). The utricular macula showed both *Irx3* and *Irx6* expression (mu in **b** and **b'**), whereas the saccular macula showed strong staining exclusively with the *Irx6* probe (ms in **b'**). In the cochlear duct, heterogeneous *Irx3* and *Irx6* expression was detected in some portions of its non-sensory parts (cd; short arrows in **c** and **d**). The basilar papilla and the lagenar macula were devoid of *Irx3* and *Irx6* mRNA (bp and ml; **c** and **d**). **e** and **f** show 3D diagrams of the *Irx3* expression pattern at stage HH34 in anterior (**e**) and posterior (**f**) views. Hatched areas show the sensory elements. For the abbreviations, see the list. Orientation: A, anterior; D, dorsal; M, medial, P, posterior. Scale bar = 170 μm in **a** (applies to **a**), 140 μm in **b** (applies to **b**), 150 μm in **b'** (applies to **b'**), and 290 μm in **d** (applies to **c** and **d**).

Figure 10. *Irx5* expression pattern at stage HH34. Horizontal sections, indicated in **e** and **f**, treated with *Irx5* probe. The sensory patches were identified by 3A10 immunoreaction. *Irx5* expression labeled the cochlear duct (arrows). Some portions of the saccular macula, the basilar papilla, and the lagenar macula were bordered by the *Irx5*-expressing domain (arrowheads). *Irx5* transcripts were not detected in any sensory patch. **e** and **f** show 3D diagrams of the *Irx5* expression pattern at stage HH34 in anterior (**e**) and posterior (**f**) views. Hatched areas show the sensory elements. For the abbreviations, see the list. Orientation: A, anterior; D, dorsal; M, medial, P, posterior. Scale bar = 160 μm in **b** (applies to **b**) and 180 μm in **c** (applies to **a**, **c**, **d**).

REFERENCES

Abelló G, Alsina B (2007) Establishment of a proneural field in the inner ear. Int J Dev Biol 51:483-493

Abelló G, Khatri S, Giráldez F, Alsina B (2007) Early regionalization of the otic placode and its regulation by the Notch signaling pathway. Mech Dev 124:631-645

Abelló G, Khatri S, Radosevic M, Scotting PJ, Giráldez F, Alsina, B (2010) Independent regulation of Sox3 and Lmx1b by FGF and BMP signaling influences the neurogenic and non-neurogenic domains in the chick otic placode. Dev Biol 339:166-178

Bao ZZ, Bruneau BG, Seidman JG, Seidman CE, Cepko CL (1999) Regulation of chamber-specific gene expression in the developing heart by Irx4. Science 283:1161-1164

Becker MB, Zulch A, Bosse A, Gruss P (2001). Irx1 and Irx2 expression in early lung development. Mech Dev 106:155-168

Bellefroid EJ, Kobbe A, Gruss P, Pieler T, Gurdon JB, Papalopulu N (1998) Xiro3 encodes a Xenopus homolog of the Drosophila Iroquois genes and functions in neural specification. EMBO J 17:191-203

Bok J, Bronner-Fraser M, Wu DK (2005) Role of the hindbrain in dorsoventral but not anteroposterior axial specification of the inner ear. Development 132:2115-2124

Bok J, Chang W, Wu DK (2007a) Patterning and morphogenesis of the vertebrate inner ear. Int J Dev Biol 51:521-533

Bok J, Dolson DK, Hill P, Ruther U, Epstein DJ, Wu DK (2007b) Opposing gradients of Gli repressor and activators mediate Shh signaling along the dorsoventral axis of the inner ear. Development 134:1713-1722

Bok J, Raft S, Kong KA, Koo SK, Drager UC, Wu DK (2011) Transient retinoic acid signaling confers anterior-posterior polarity to the inner ear. Proc Natl Acad Sci U S A 108:161-166

Bosse A, Stoykova A, Nieselt-Struwe K, Chowdhury K, Copeland NG, Jenkins NA, Gruss P (2000) Identification of a novel mouse Iroquois homeobox gene, Irx5, and chromosomal localisation of all members of the mouse Iroquois gene family. Dev Dyn 218:160-174

Bosse A, Zulch A, Becker MB, Torres M, Gómez-Skarmeta JL, Modolell J, Gruss P (1997) Identification of the vertebrate Iroquois homeobox gene family with overlapping expression during early development of the nervous system. Mech Dev 69:169-181

Brigande JV, Kiernan AE, Gao X, Iten LE, Fekete DM (2000) Molecular genetics of pattern formation in the inner ear: do compartment boundaries play a role? Proc Natl Acad Sci U S A 97:11700-11706

Briscoe J, Ericson J (2001) Specification of neuronal fates in the ventral neural tube. Curr Opin Neurobiol 11:43-49

Briscoe J, Pierani A, Jessell TM, Ericson J, (2000) A homeodomain protein code specifies progenitor cell identity and neuronal fate in the ventral neural tube. Cell 101:435-445

Bruneau BG, Bao ZZ, Fatkin D, Xavier-Neto J, Georgakopoulos D, Maguire CT, Berul, CI, Kass DA, Kuroski-de Bold ML, de Bold AJ, Conner D A, Rosenthal N, Cepko CL, Seidman CE, Seidman JG (2001) Cardiomyopathy in Irx4-deficient mice is preceded by abnormal ventricular gene expression. Mol Cell Biol 21:1730-1736

Bürglin TR (1997) Analysis of TALE superclass homeobox genes (MEIS, PBC, KNOX, Iroquois, TGIF) reveals a novel domain conserved between plants and animals. Nucleic Acids Res 25:4173-4180

Calleja M, Renaud O, Usui K, Pistillo D, Morata G, Simpson P (2002) How to pattern an epithelium: lessons from achaete-scute regulation on the notum of Drosophila. Gene 292:1-12

Cantos R, Cole LK, Acampora D, Simeone A, Wu DK (2000) Patterning of the mammalian cochlea. Proc Natl Acad Sci U S A 97:11707-1713

Casarosa S, Andreazzoli M, Simeone A, Barsacchi G (1997) Xrx1, a novel Xenopus homeobox gene expressed during eye and pineal gland development. Mech Dev 61:187-198

Cavodeassi F, Díez-del-Corral R, Campuzano S, Domínguez M (1999) Compartments and organising boundaries in the Drosophila eye: the role of the homeodomain Iroquois proteins. Development 126:4933-4942

Cavodeassi F, Modolell J, Gómez-Skarmeta JL (2001) The Iroquois family of genes: from body building to neural patterning. Development 128:2847-2855

Cavodeassi F, Rodríguez I, Modolell J (2002) Dpp signalling is a key effector of the wing-body wall subdivision of the Drosophila mesothorax. Development 129:3815-3823

Chatterjee S, Kraus P, Lufkin T (2010) A symphony of inner ear developmental control genes. BMC Genet 11:68

Chen J, Streit A (2013) Induction of the inner ear: stepwise specification of otic fate from multipotent progenitors. Hear Res 297:3-12

Cheng CW, Chow RL, Lebel M, Sakuma R, Cheung HO, Thanabalasingham V, Zhang X, Bruneau BG, Birch DG, Hui CC, McInnes RR, Cheng SH (2005) The Iroquois homeobox gene, Irx5, is required for retinal cone bipolar cell development. Dev Biol 287:48-60

Cheng CW, Yan CH, Choy SW, Hui MN, Hui CC, Cheng SH (2007) Zebrafish homologue irx1a is required for the differentiation of serotonergic neurons. Dev Dyn 236:2661-2267

Cheng CW, Yan CH, Hui CC, Strahle U, Cheng SH (2006) The homeobox gene irx1a is required for the propagation of the neurogenic waves in the zebrafish retina. Mech Dev 123:252-263

Christoffels VM, Keijser AG, Houweling AC, Clout DE, Moorman AF (2000) Patterning the embryonic heart: identification of five mouse Iroquois homeobox genes in the developing heart. Dev Biol 224:263-274

Cohen DR, Cheng CW, Cheng SH, Hui CC (2000) Expression of two novel mouse Iroquois homeobox genes during neurogenesis. Mech Dev 91:317-321

Constantini DL, Arruda EP, Agarwal P, Kim KH, Zhu Y, Zhu W, Lebel M, Cheng CW, Park CY, Pierce SA, Guerchicoff A, Pollevick GD, Chan TY, Kabir MG, Cheng SH, Husain M, Antzelevitch C, Srivastava D, Gross GJ, Hui CC, Backx PH, Bruneau BG (2005) The homeodomain transcription factor Irx5 establishes the mouse cardiac ventricular repolarization gradient. Cell 123:347-358

de la Calle-Mustienes E, Feijóo CG, Manzanares M, Tena JJ, Rodríguez-Seguel E, Letizia A, Allende ML, Gómez-Skarmeta JL (2005) A functional survey of the enhancer activity of conserved non-coding sequences from vertebrate Iroquois cluster gene deserts. Genome Res 15:1061-1072

Díaz-Hernández ME, Bustamante M, Galván-Hernández CI, Chimal-Monroy J (2013) Irx1 and Irx2 are coordinately expressed and regulated by retinoic acid, TGFbeta and FGF signaling during chick hindlimb development. PLoS One 8:e58549

Díez-del-Corral R, Aroca P, Gómez-Skarmeta, JL, Cavodeassi F, Modolell J (1999) The Iroquois homeodomain proteins are required to specify body wall identity in Drosophila. Genes Dev 13:1754-1761

Díez-del-Corral R, Olivera-Martínez I, Goriely A, Gale E, Maden M, Storey K (2003) Opposing FGF and retinoid pathways control ventral neural pattern, neuronal differentiation, and segmentation during body axis extension. Neuron 40:65-79

Dildrop R, Ruther U (2004) Organization of Iroquois genes in fish. Dev Genes Evol 214:267-276

Domínguez M, de Celis JF (1998) A dorsal/ventral boundary established by Notch controls growth and polarity in the Drosophila eye. Nature 396:276-278

Ekker M, Akimenko MA, Bremiller R, Westerfield M (1992) Regional expression of three homeobox transcripts in the inner ear of zebrafish embryos. Neuron 9:27-35

El-Dahr SS, Aboudehen K, Saifudeen Z (2008). Transcriptional control of terminal

nephron differentiation. Am J Physiol Renal Physiol 294:F1273-1278

Feijóo CG, Manzanares M, de la Calle-Mustienes E, Gómez-Skarmeta JL, Allende ML (2004) The Irx gene family in zebrafish: genomic structure, evolution and initial characterization of irx5b. Dev Genes Evol 214:277-284

Feijóo CG, Saldias MP, de la Paz JF, Gómez-Skarmeta JL, Allende, ML (2009) Formation of posterior cranial placode derivatives requires the Iroquois transcription factor irx4a. Mol Cell Neurosci 40:328-337

Fekete DM (1996) Cell fate specification in the inner ear. Curr Opin Neurobiol 6:533-541

Fekete DM, Campero AM (2007) Axon guidance in the inner ear. Int J Dev Biol 51:549-556

Fekete DM, Wu DK (2002) Revisiting cell fate specification in the inner ear. Curr Opin Neurobiol 12:35-42

Ferran JL, Ayad A, Merchán P, Morales-Delgado N, Sánchez-Arrones L, Alonso A, Sandoval JE, Bardet SM, Corral-San-Miguel R, Sánchez-Guardado LO, Hidalgo-Sánchez M, Martínez-de-la-Torre M, Puelles, L (2015) Exploring *brain genoarchitecture* by single and double chromogenic *in situ* hybridization (ISH) and immunohistochemistry (IHC) on cryostat, paraffin, or floating sections. In: Hauptmann G (ed.) In situ hybridization Methods. Springer Protocols, Berlin, Springer Science + Business Media, pp 83-107

Frenz DA, Liu W, Cvekl A, Xie Q, Wassef L, Quadro L, Niederreither K, Maconochie M, Shanske A (2010) Retinoid signaling in inner ear development: A "Goldilocks" phenomenon. Am J Med Genet A 152A:2947-2961

Gaborit N, Sakuma R, Wylie JN, Kim KH, Zhang SS, Hui CC, Bruneau BG (2012) Cooperative and antagonistic roles for Irx3 and Irx5 in cardiac morphogenesis and postnatal physiology. Development 139:4007-4019

García-Campmany L, Martí E (2007) The TGFbeta intracellular effector Smad3 regulates neuronal differentiation and cell fate specification in the developing spinal

cord. Development 134:65-75

Glavic A, Gómez-Skarmeta JL, Mayor R (2001) Xiro-1 controls mesoderm patterning by repressing bmp-4 expression in the Spemann organizer. Dev Dyn 222:368-376

Glavic A, Gómez-Skarmeta JL, Mayor R (2002) The homeoprotein Xiro1 is required for midbrain-hindbrain boundary formation. Development 129:1609-1621

Glavic A, Maris-Honore S, Gloria-Feijóo, C, Bastidas F, Allende ML, Mayor R (2004) Role of BMP signaling and the homeoprotein Iroquois in the specification of the cranial placodal field. Dev Biol 272:89-103

Gómez-Skarmeta JL, Díez-del-Corral R, de la Calle-Mustienes E, Ferre-Marco D, Modolell J (1996) Araucan and caupolican, two members of the novel iroquois complex, encode homeoproteins that control proneural and vein-forming genes. Cell 85:95-105

Gómez-Skarmeta JL, Glavic A, de la Calle-Mustienes E, Modolell J, Mayor R (1998) Xiro, a Xenopus homolog of the Drosophila Iroquois complex genes, controls development at the neural plate. EMBO J 17:181-190

Gómez-Skarmeta JL, Modolell J (2002) Iroquois genes: genomic organization and function in vertebrate neural development. Curr Opin Genet Dev 12:403-408

Goriely A, Díez-del-Corral R, Storey KG (1999) c-Irx2 expression reveals an early subdivision of the neural plate in the chick embryo. Mech Dev 87:203-206

Groves AK, Fekete DM (2012) Shaping sound in space: the regulation of inner ear patterning. Development 139:245-257

.

Hamburger V, Hamilton HL (1951) A series of normal stages in the development of the chick embryo. J Morphol 88:49-92

Hammond KL, Whitfield TT (2011) Fgf and Hh signalling act on a symmetrical pre-pattern to specify anterior and posterior identity in the zebrafish otic placode and vesicle. Development 138:3977-3987

Hidalgo-Sanchez M, Alvarado-Mallart R, Alvarez IS (2000) Pax2, Otx2, Gbx2 and Fgf8 expression in early otic vesicle development. Mech Dev 95:225-229

Hidalgo-Sánchez M, Millet S, Bloch-Gallego E, Alvarado-Mallart RM (2005a) Specification of the meso-isthmo-cerebellar region: the Otx2/Gbx2 boundary. Brain Res Brain Res Rev 49:134-149

Hidalgo-Sánchez M, Martínez-De-La-Torre M, Alvarado-Mallart R-M, Puelles L (2005b) A distinct preisthmic histogenetic domain is defined by overlap of *Otx2* and *Pax2* gene expression in the avian caudal midbrain. J Comp Neurol 483:17–29

Hirata T, Nakazawa M, Muraoka O, Nakayama R, Suda Y, Hibi M (2006) Zinc-finger genes Fez and Fez-like function in the establishment of diencephalon subdivisions. Development 133:3993-4004

Houweling AC, Dildrop R, Peters T, Mummenhoff J, Moorman AF, Ruther U, Christoffels VM (2001) Gene and cluster-specific expression of the Iroquois family members during mouse development. Mech Dev 107:169-174

Ikmi A, Netter S, Coen D (2008) Prepatterning the Drosophila notum: the three genes of the iroquois complex play intrinsically distinct roles. Dev Biol 317:634-648

Irimia M, Maeso I, García-Fernández J (2008) Convergent evolution of clustering of Iroquois homeobox genes across metazoans. Mol Biol Evol 25:1521-1525

Itoh M, Kudoh T, Dedekian M, Kim CH, Chitnis AB (2002) A role for iro1 and iro7 in the establishment of an anteroposterior compartment of the ectoderm adjacent to the midbrain-hindbrain boundary. Development 129:2317-2327

Jin Z, Zhang J, Klar A, Chedotal A, Rao Y, Cepko CL, Bao ZZ (2003) Irx4-mediated regulation of Slit1 expression contributes to the definition of early axonal paths inside the retina. Development 130:1037-1048

Jorgensen JS, Gao L (2005) Irx3 is differentially up-regulated in female gonads during sex determination. Gene Expr Patterns 5:756-762

Joseph EM (2004) Zebrafish IRX1b in the embryonic cardiac ventricle. Dev Dyn 231:720-726

Kehl BT, Cho KO, Choi KW (1998) mirror, a Drosophila homeobox gene in the Iroquois complex, is required for sensory organ and alula formation. Development 125:1217-1227

Kelly MC, Chen P (2009) Development of form and function in the mammalian cochlea. Curr Opin Neurobiol 19:395-401

Kerner P, Ikmi A, Coen D, Vervoort M (2009) Evolutionary history of the iroquois/Irx genes in metazoans. BMC Evol Biol 9:74

Kiecker C, Lumsden A (2004) Hedgehog signaling from the ZLI regulates diencephalic regional identity. Nat Neurosci 7:1242-1249

Kim KH, Rosen A, Bruneau BG, Hui CC, Backx PH (2012) Iroquois homeodomain transcription factors in heart development and function. Circ Res 110:1513-1524

Kobayashi D, Kobayashi M, Matsumoto K, Ogura T, Nakafuku M, Shimamura K (2002) Early subdivisions in the neural plate define distinct competence for inductive signals. Development 129:83-93

Kojima T, Asano S, Takahashi, N (2013) Teratogenic factors affect transcription factor expression. Biosci Biotechnol Biochem 77:1035-1041

Kudoh T, Dawid IB (2001) Role of the iroquois3 homeobox gene in organizer formation. Proc Natl Acad Sci U S A 98:7852-7857

Ladher RK, O'Neill P, Begbie J (2010) From shared lineage to distinct functions: the development of the inner ear and epibranchial placodes. Development 137:1777-1785

Larroux C, Luke GN, Koopman P, Rokhsar DS, Shimeld SM, Degnan BM (2008) Genesis and expansion of metazoan transcription factor gene classes. Mol Biol Evol 25:980-996

Lebel M, Agarwal P, Cheng CW, Kabir MG, Chan TY, Thanabalasingham V, Zhang X,

Cohen DR, Husain M, Cheng SH, Bruneau BG, Hui CC (2003) The Iroquois homeobox gene Irx2 is not essential for normal development of the heart and midbrain-hindbrain boundary in mice. Mol Cell Biol 23:8216-8225

Lecaudey V, Anselme I, Dildrop R, Ruther U, Schneider-Maunoury S (2005) Expression of the zebrafish Iroquois genes during early nervous system formation and patterning. J Comp Neurol 492:289-302

Lecaudey V, Anselme I, Rosa F, Schneider-Maunoury S (2004) The zebrafish Iroquois gene iro7 positions the r4/r5 boundary and controls neurogenesis in the rostral hindbrain. Development 131:3121-3131

Lin Z, Cantos R, Patente M, Wu DK (2005) Gbx2 is required for the morphogenesis of the mouse inner ear: a downstream candidate of hindbrain signaling. Development 132:2309-2318

Liu Y, Liu C, Yamada Y, Fan CM (2002) Growth arrest specific gene 1 acts as a region-specific mediator of the Fgf10/Fgf8 regulatory loop in the limb. Development 129:5289-5300

López-Sánchez C, Bartulos O, Martínez-Campos E, Ganan C, Valenciano AI, García-Martínez V, De Pablo F, Hernández-Sánchez C (2010) Tyrosine hydroxylase is expressed during early heart development and is required for cardiac chamber formation. Cardiovasc Res 88:111-120

Matsumoto K, Nishihara S, Kamimura M, Shiraishi T, Otoguro T, Uehara M, Maeda Y, Ogura K, Lumsden A, Ogura T (2004) The prepattern transcription factor Irx2, a target of the FGF8/MAP kinase cascade, is involved in cerebellum formation. Nat Neurosci 7:605-612

McNeill H, Yang CH, Brodsky M, Ungos J, Simon MA (1997). mirror encodes a novel PBX-class homeoprotein that functions in the definition of the dorsal-ventral border in the Drosophila eye. Genes Dev 11:1073-1082

Mukherjee K, Bürglin TR (2007) Comprehensive analysis of animal TALE homeobox genes: new conserved motifs and cases of accelerated evolution. J Mol Evol 65:137-153

Mummenhoff J, Houweling AC, Peters T, Christoffels VM, Ruther U (2001) Expression of Irx6 during mouse morphogenesis. Mech Dev 103:193-195

Novitch BG, Chen AI, Jessell TM (2001). Coordinate regulation of motor neuron subtype identity and pan-neuronal properties by the bHLH repressor Olig2. Neuron 31:773-789

Ogura K, Matsumoto K, Kuroiwa A, Isobe T, Otoguro T, Jurecic V, Baldini A, Matsuda Y, Ogura T (2001) Cloning and chromosome mapping of human and chicken Iroquois (IRX) genes. Cytogenet Cell Genet 92:320-325

Oh SH, Johnson R, Wu DK (1996) Differential expression of bone morphogenetic proteins in the developing vestibular and auditory sensory organs. J Neurosci 16:6463-6475

Ohyama T, Groves AK, Martin K (2007) The first steps towards hearing: mechanisms of otic placode induction. Int J Dev Biol 51:463-472

Ozaki H, Nakamura K, Funahashi J, Ikeda K, Yamada G, Tokano H, Okamura HO, Kitamura K, Muto S, Kotaki H, Sudo K, Horai R, Iwakura Y, Kawakami K (2004) Six1 controls patterning of the mouse otic vesicle. Development 131:551-562

Papayannopoulos V, Tomlinson A, Panin VM, Rauskolb C, Irvine KD (1998). Dorsal-ventral signaling in the Drosophila eye. Science 281:2031-2034

Perovic S, Schroder HC, Sudek S, Grebenjuk VA, Batel R, Stifanic M, Muller IM, Muller WE (2003) Expression of one sponge Iroquois homeobox gene in primmorphs from Suberites domuncula during canal formation. Evol Dev 5:240-250

Peters T, Dildrop R, Ausmeier K, Ruther U (2000) Organization of mouse Iroquois homeobox genes in two clusters suggests a conserved regulation and function in vertebrate development. Genome Res 10:1453-1462

Pichaud F, Casares F (2000) homothorax iroquois-C genes are required for the establishment of territories within the developing eye disc. Mech Dev 96:15-25

Pose-Méndez S, Candal E, Mazan S, Rodríguez-Moldes I (2015) Genoarchitecture of the rostral hindbrain of a shark: basis for understanding the emergence of the cerebellum at the agnathan-gnathostome transition. Brain Struct Funct pp 1-15

Reggiani L, Raciti D, Airik R, Kispert A, Brandli AW (2007) The prepattern transcription factor Irx3 directs nephron segment identity. Genes Dev 21:2358-2370

Riccomagno MM, Martinu L, Mulheisen M, Wu DK, Epstein DJ (2002). Specification of the mammalian cochlea is dependent on Sonic hedgehog. Genes Dev 16:2365-2378

Riccomagno MM, Takada S, Epstein DJ (2005) Wnt-dependent regulation of inner ear morphogenesis is balanced by the opposing and supporting roles of Shh. Genes Dev 19:1612-1623

Rodríguez-Seguel E, Alarcon P, Gómez-Skarmeta JL (2009) The Xenopus Irx genes are essential for neural patterning and define the border between prethalamus and thalamus through mutual antagonism with the anterior repressors Fezf and Arx. Dev Biol 329:258-268

Romand R, Dolle P, Hashino E (2006) Retinoid signaling in inner ear development. J Neurobiol 66:687-704

Sánchez-Calderón H, Martin-Partido G, Hidalgo-Sánchez M (2002) Differential expression of Otx2, Gbx2, Pax2, and Fgf8 in the developing vestibular and auditory sensory organs. Brain Res Bull 57:321-323

Sánchez-Calderón H, Martín-Partido G, Hidalgo-Sánchez M (2004) Otx2, Gbx2, and Fgf8 expression patterns in the chick developing inner ear and their possible roles in otic specification and early innervation. Gene Expr Patterns 4:659-669

Sánchez-Calderón H, Martín-Partido G, Hidalgo-Sánchez M (2005) Pax2 expression patterns in the developing chick inner ear. Gene Expr Patterns 5:763-773.

Sánchez-Calderón H, Milo M, León Y, Varela-Nieto I (2007a) A network of growth and transcription factors controls neuronal differentation and survival in the developing ear. Int J Dev Biol 51:557-570

Sánchez-Calderón H, Francisco-Morcillo J, Martin-Partido G, Hidalgo-Sánchez M (2007b) Fgf19 expression patterns in the developing chick inner ear. Gene Expr Patterns 7:30-38

Sánchez-Guardado LO, Ferran JL, Mijares J, Puelles L, Rodríguez-Gallardo L, Hidalgo-Sánchez M (2009) Raldh3 gene expression pattern in the developing chicken inner ear. J Comp Neurol 514:49-65

Sánchez-Guardado LO, Ferran JL, Rodríguez-Gallardo L, Puelles L, Hidalgo-Sánchez M (2011) Meis gene expression patterns in the developing chicken inner ear. J Comp Neurol 519:125-147

Sánchez-Guardado LO, Puelles L, Hidalgo-Sánchez M (2013) Fgf10 expression patterns in the developing chick inner ear. J Comp Neurol 521:1136-1164

Sánchez-Guardado LO, Puelles L, Hidalgo-Sánchez M (2014) Fate map of the chicken otic placode. Development 141:2302-2312

Sato T, Araki I, Nakamura H (2001) Inductive signal and tissue responsiveness defining the tectum and the cerebellum. Development 128, 2461-2469

Schimmang T (2007) Expression and functions of FGF ligands during early otic development. Int J Dev Biol 51:473-481

Schlosser G (2005) Induction and specification of cranial placodes. Dev Biol 294:303-351

Schlosser G (2006) Induction and specification of cranial placodes. Dev Biol 294:303-351.

Schlosser G, Ahrens K (2004) Molecular anatomy of placode development in Xenopus laevis. Dev Biol 271:439-466

Schneider-Maunoury S, Pujades C (2007) Hindbrain signals in otic regionalization: walk on the wild side. Int J Dev Biol 51:495-506

Stedman A, Lecaudey V, Havis E, Anselme I, Wassef M, Gilardi-Hebenstreit P,

Schneider-Maunoury S (2009) A functional interaction between Irx and Meis patterns the anterior hindbrain and activates krox20 expression in rhombomere 3. Dev Biol 327:566-577

Tan JT, Korzh V, Gong Z (1999) Expression of a zebrafish iroquois homeobox gene, Ziro3, in the midline axial structures and central nervous system. Mech Dev 87:165-181

Tena JJ, Alonso ME, de la Calle-Mustienes E, Splinter E, de Laat W, Manzanares M, Gómez-Skarmeta JL (2011) An evolutionarily conserved three-dimensional structure in the vertebrate Irx clusters facilitates enhancer sharing and coregulation. Nat Commun 2:310

Thompson DL, Gerlach-Bank LM, Barald KF, Koenig RJ (2003) Retinoic acid repression of bone morphogenetic protein 4 in inner ear development. Mol Cell Biol 23:2277-2286

Villa-Cuesta E, Modolell J (2005) Mutual repression between msh and Iro-C is an essential component of the boundary between body wall and wing in Drosophila. Development 132:4087-4096

Wassarman KM, Lewandoski M, Campbell K, Joyner AL, Rubenstein JL, Martínez S, Martin GR (1997) Specification of the anterior hindbrain and establishment of a normal mid/hindbrain organizer is dependent on Gbx2 gene function. Development 124:2923-2934

Whitfield TT, Hammond KL (2007) Axial patterning in the developing vertebrate inner ear. Int J Dev Biol 51:507-520

Wu DK, Oh SH (1996) Sensory organ generation in the chick inner ear. J Neurosci 16:6454-6462

Yang CH, Simon MA, McNeill H (1999) mirror controls planar polarity and equator formation through repression of fringe expression and through control of cell affinities. Development 126, 5857-5866

Zheng W, Huang L, Wei ZB, Silvius D, Tang B, Xu PX (2003) The role of Six1 in mammalian auditory system development. Development 130, 3989-4000

Zülch A, Becker MB, Gruss P (2001) Expression pattern of Irx1 and Irx2 during mouse digit development. Mech Dev 106, 159-162

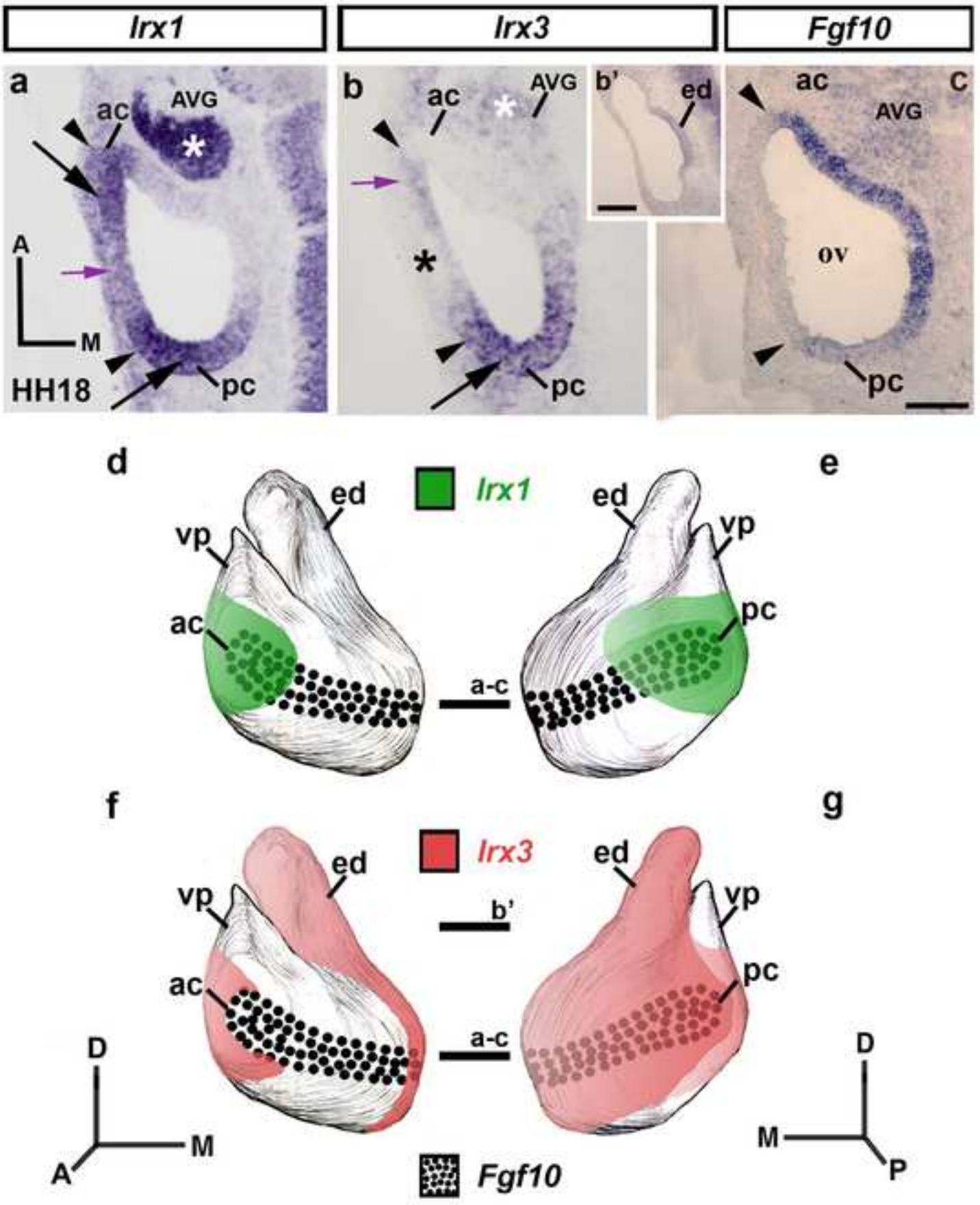

Figure 1

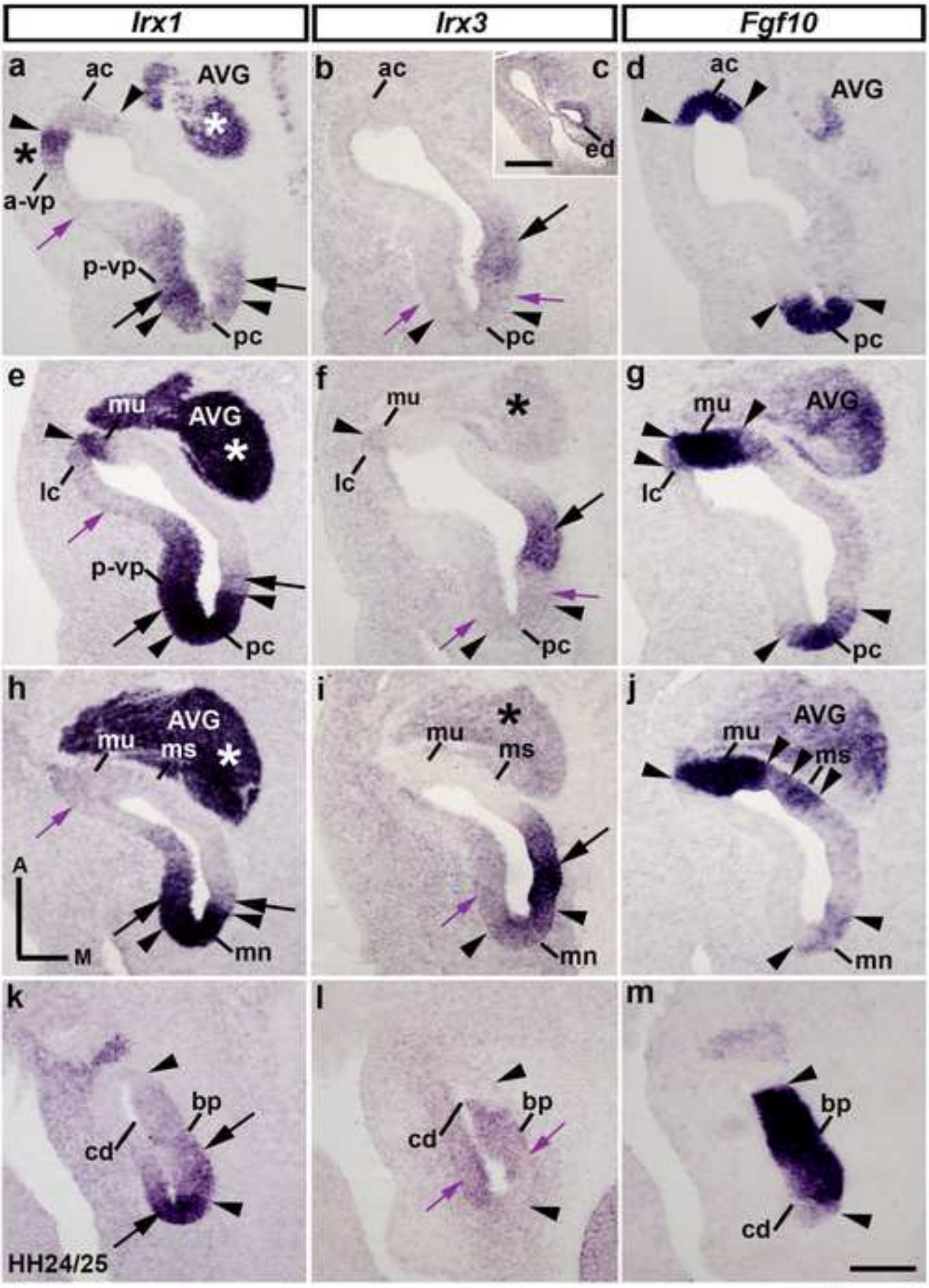

Figure 2

Figure 3

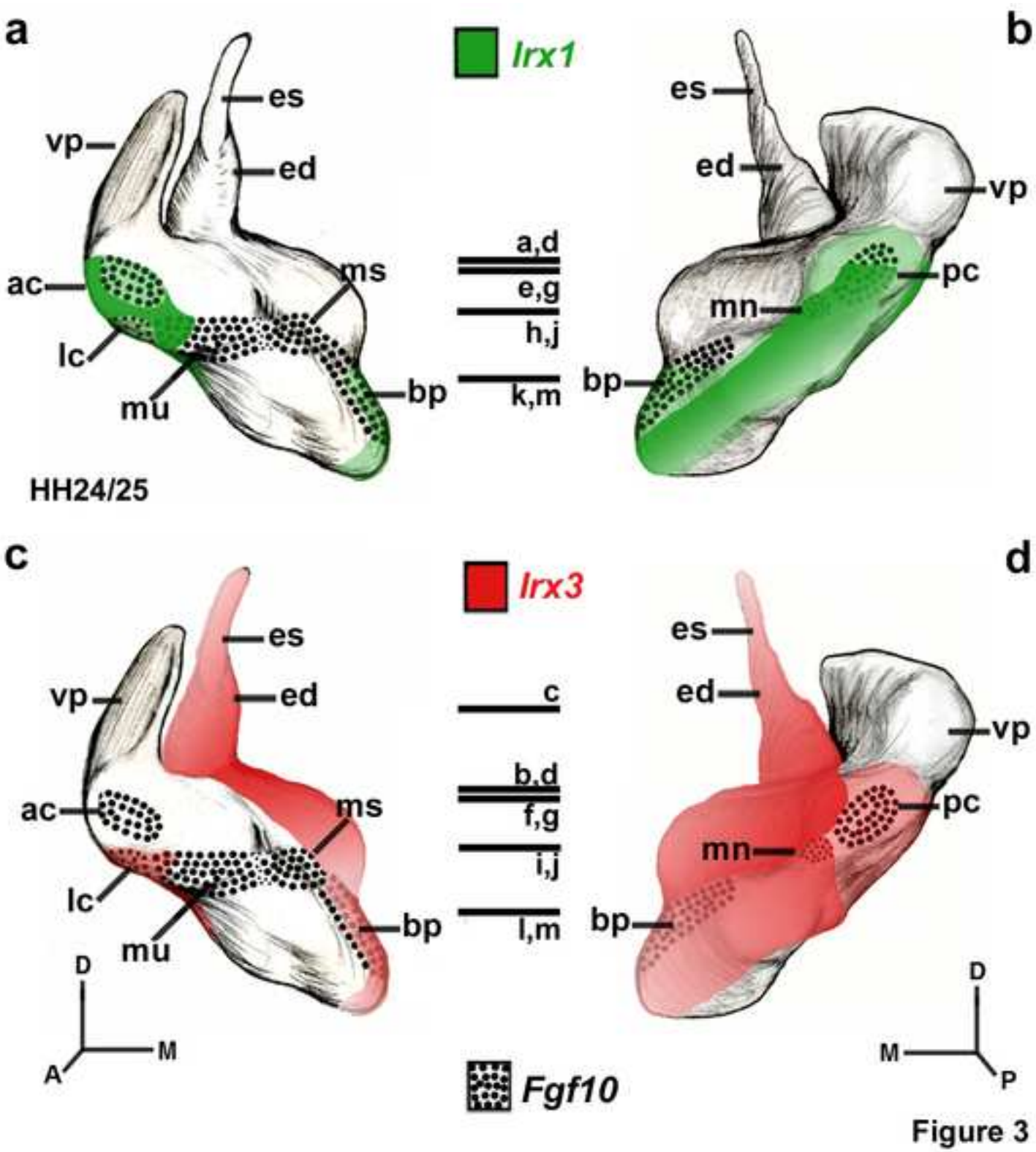

Figure 3

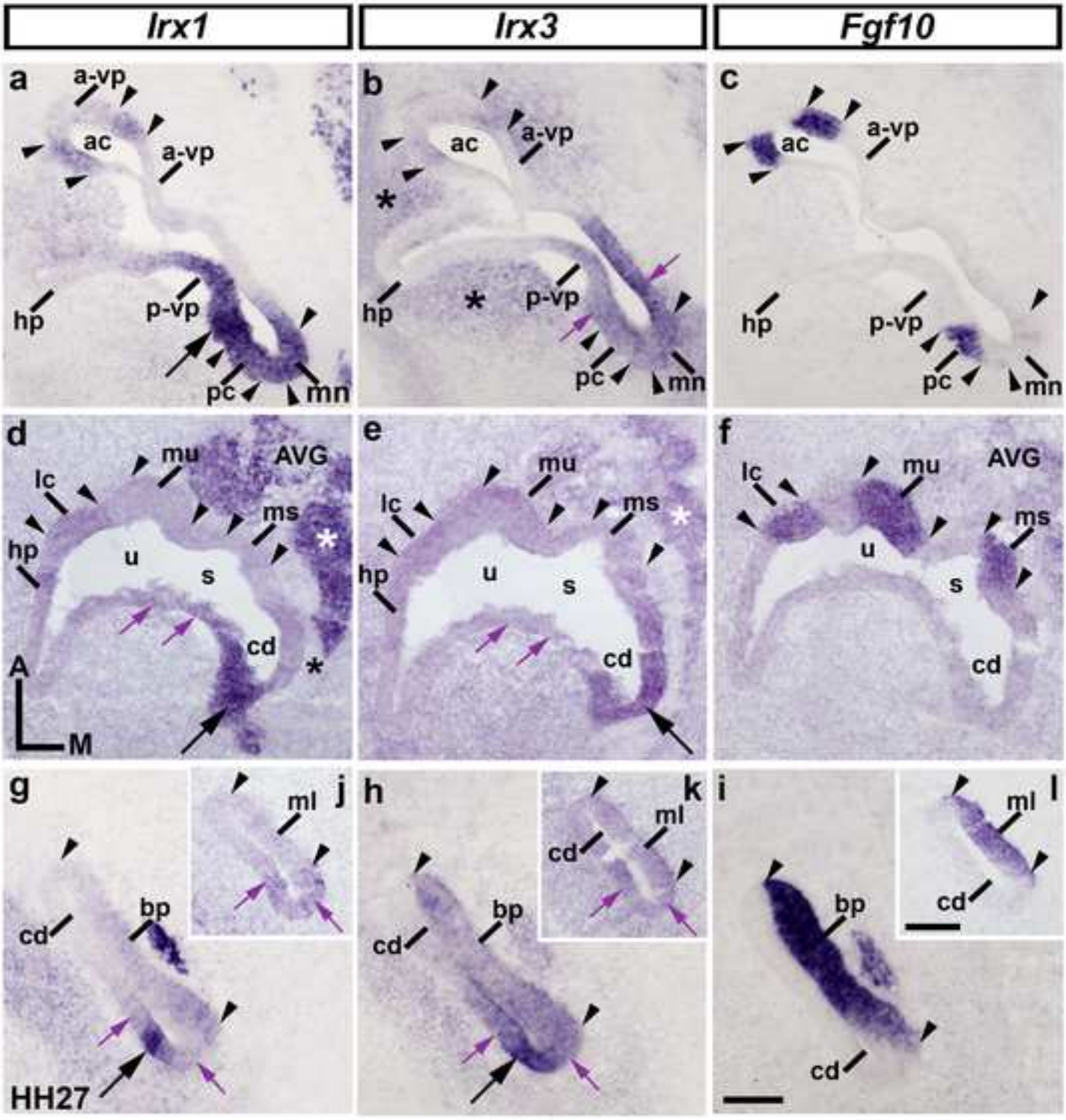

Figure 4

Figure 5

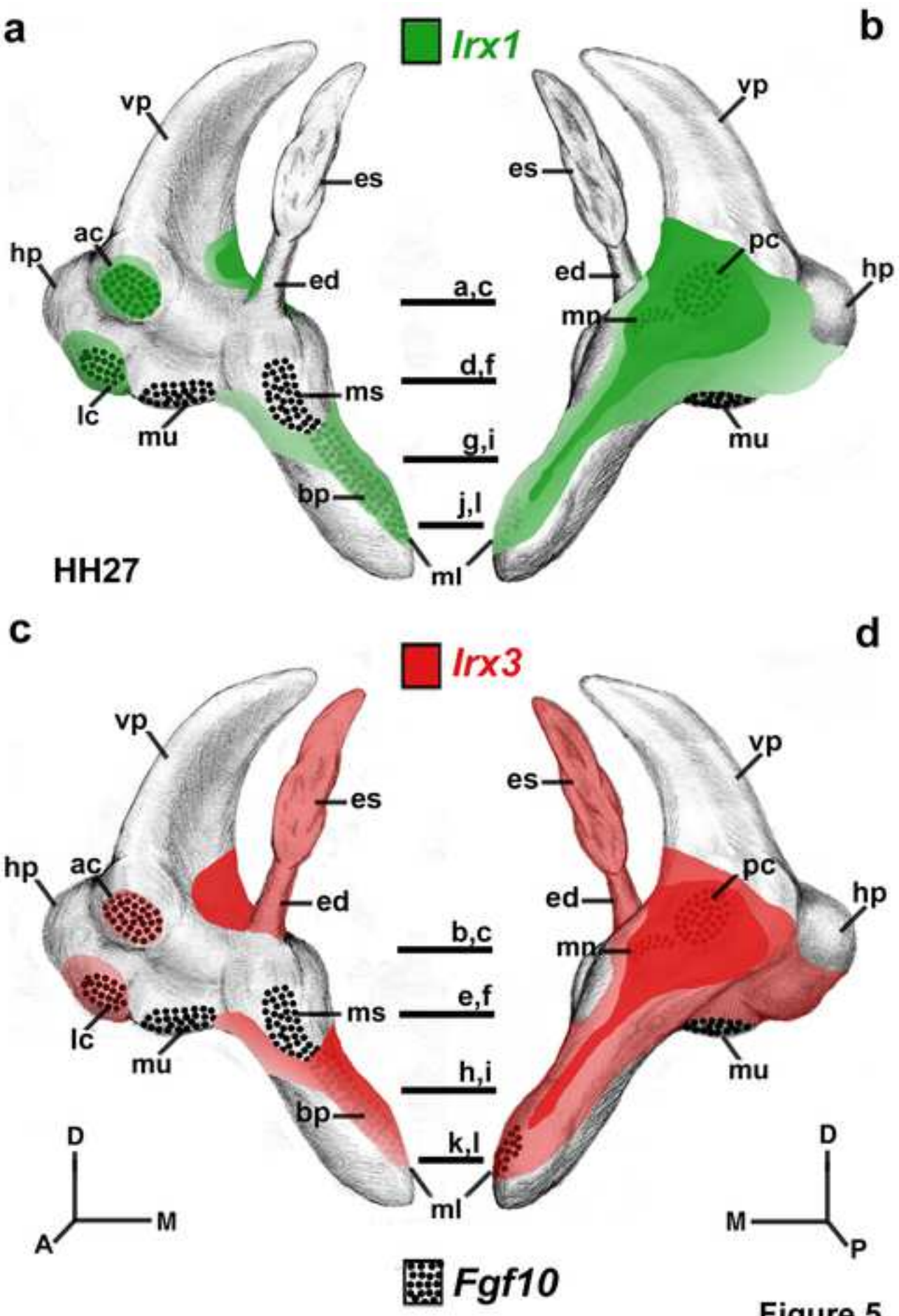

Figure 5

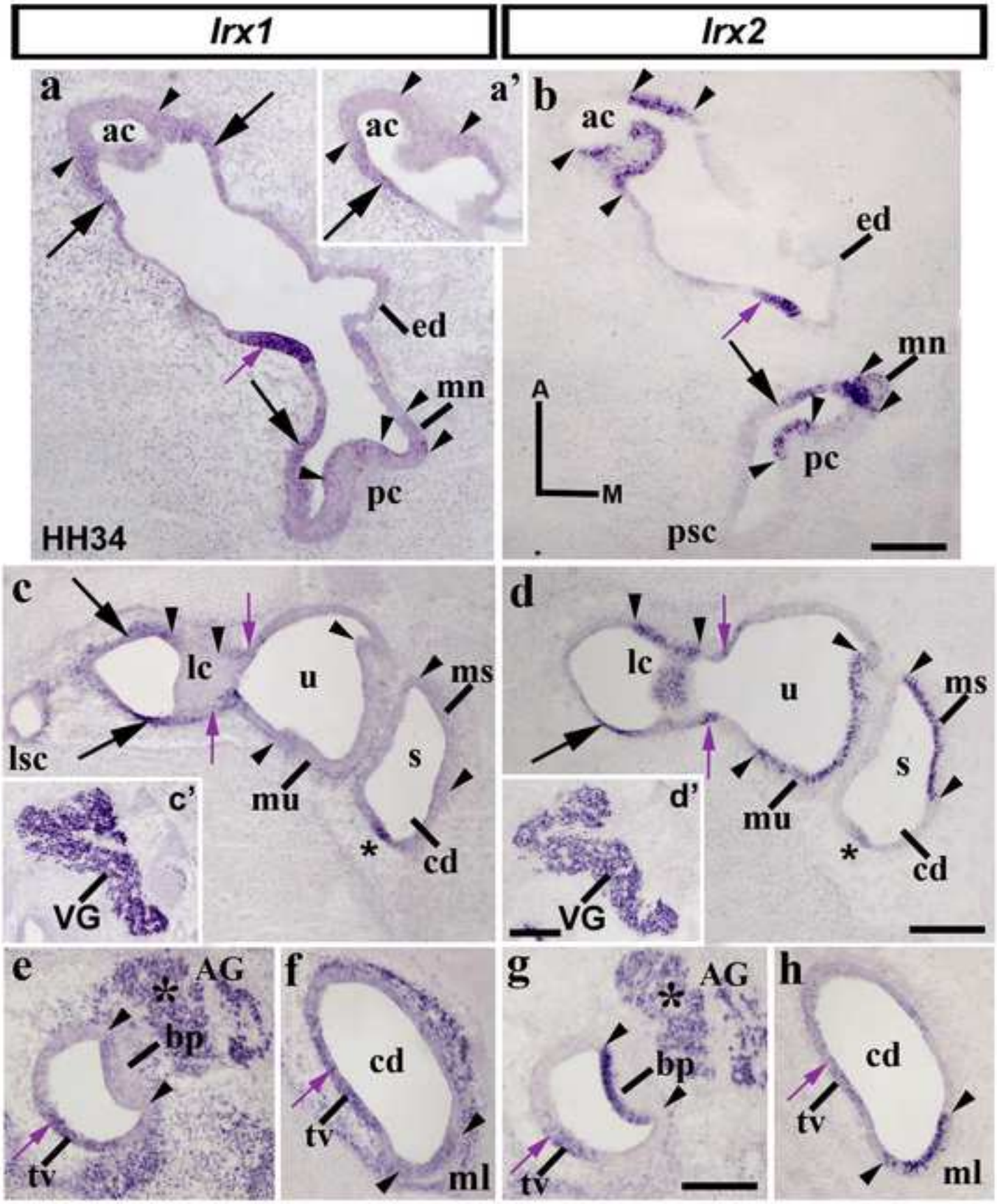

Figure 6

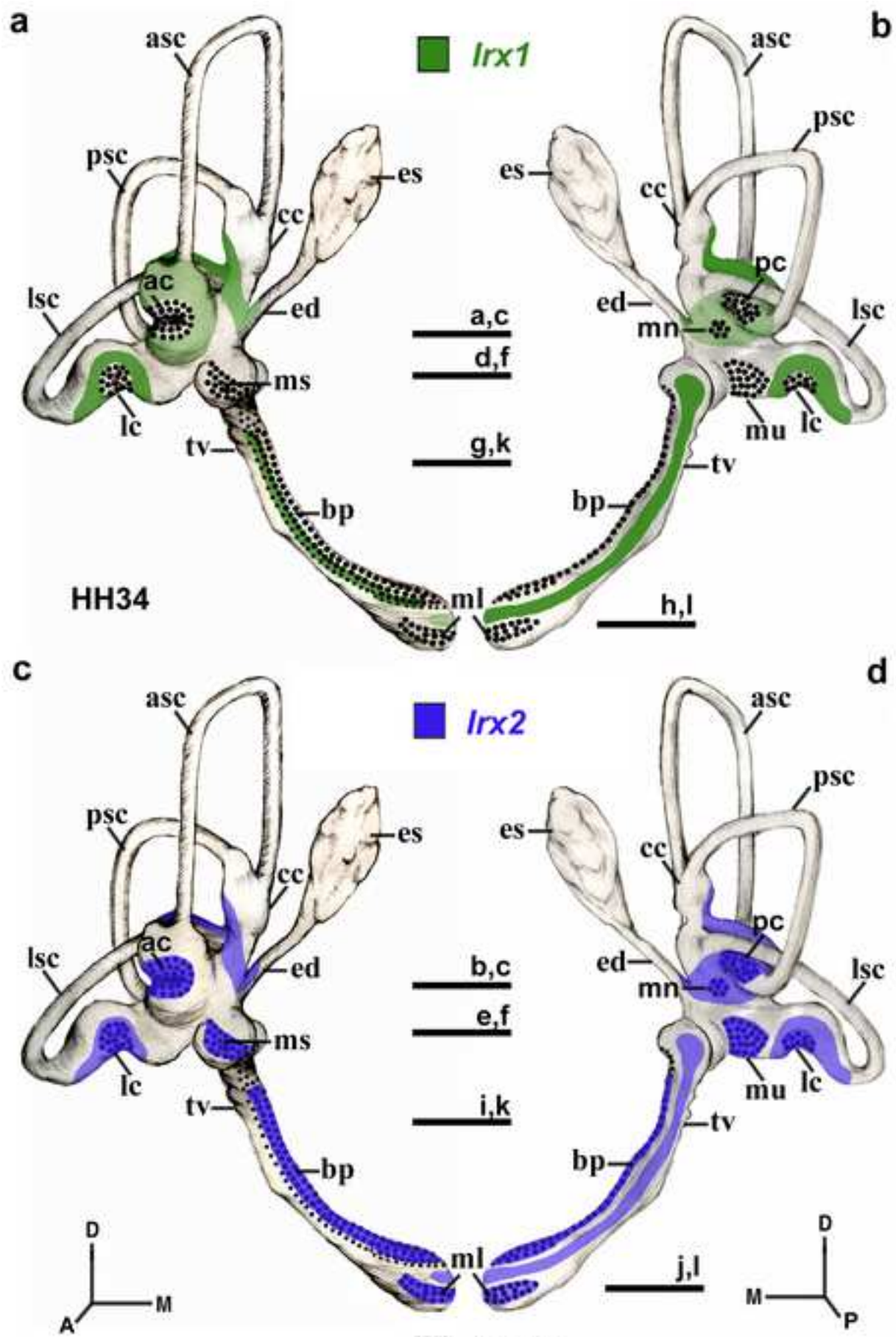

Figure 7

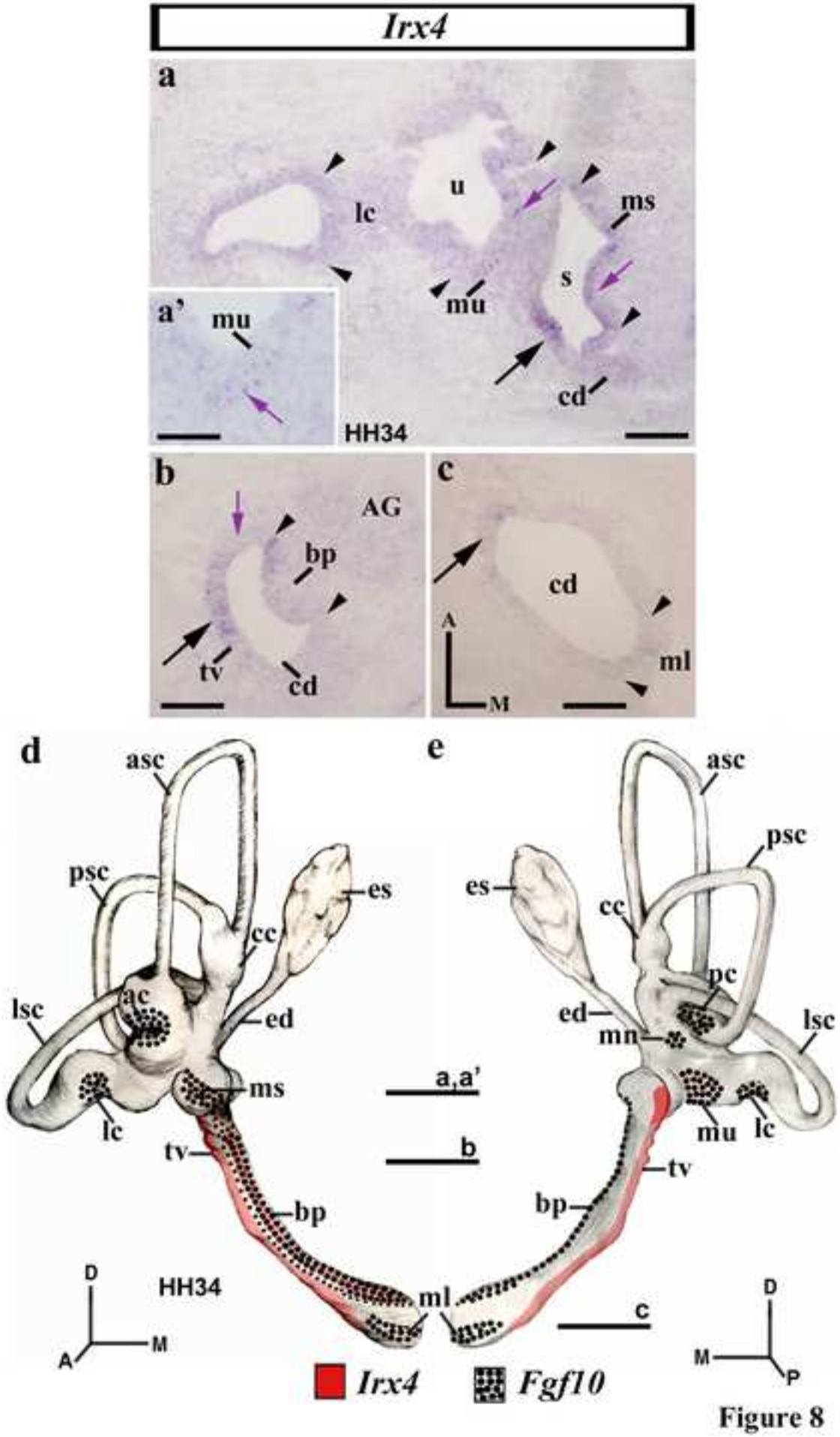

Figure 8

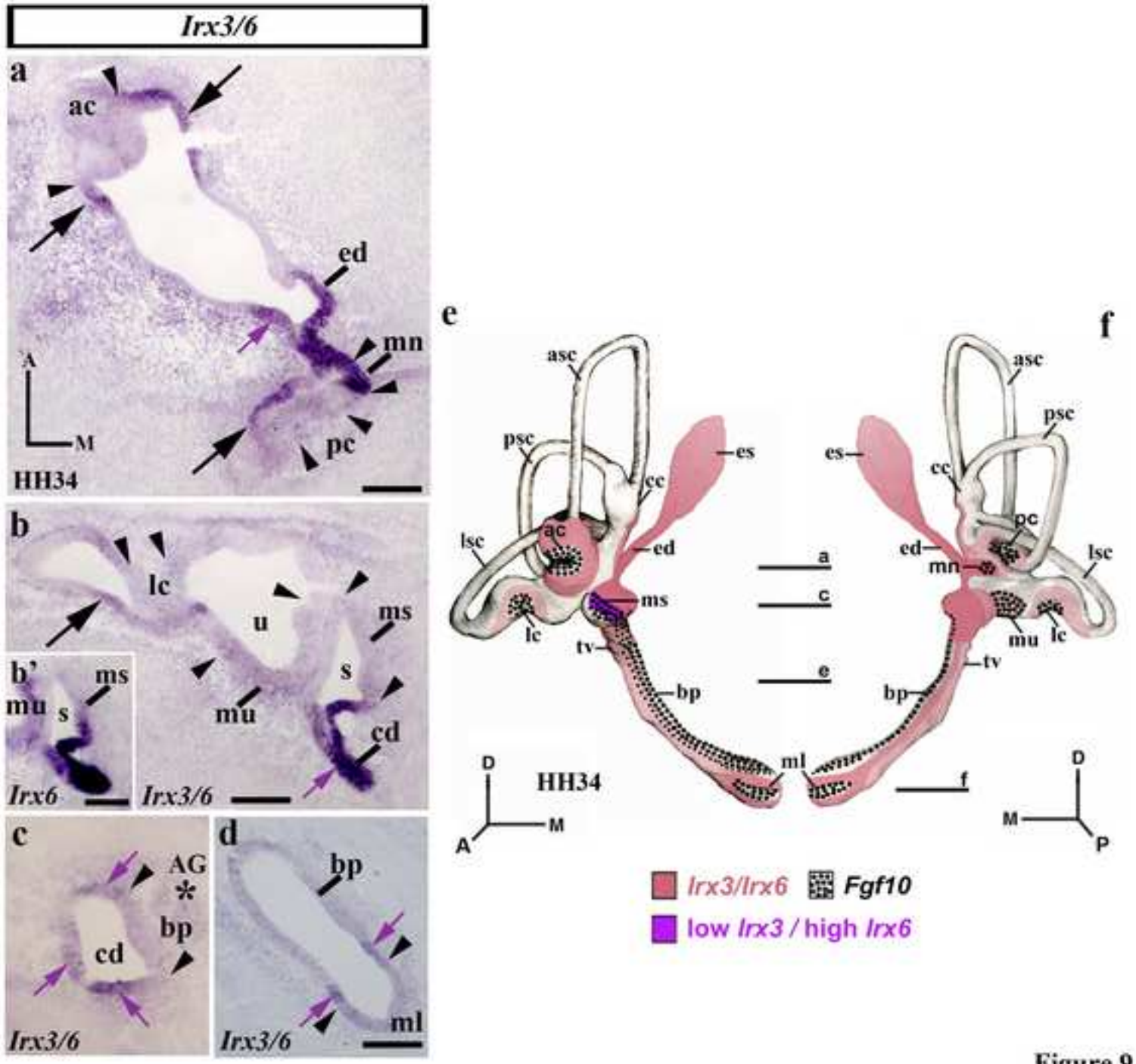

Figure 9

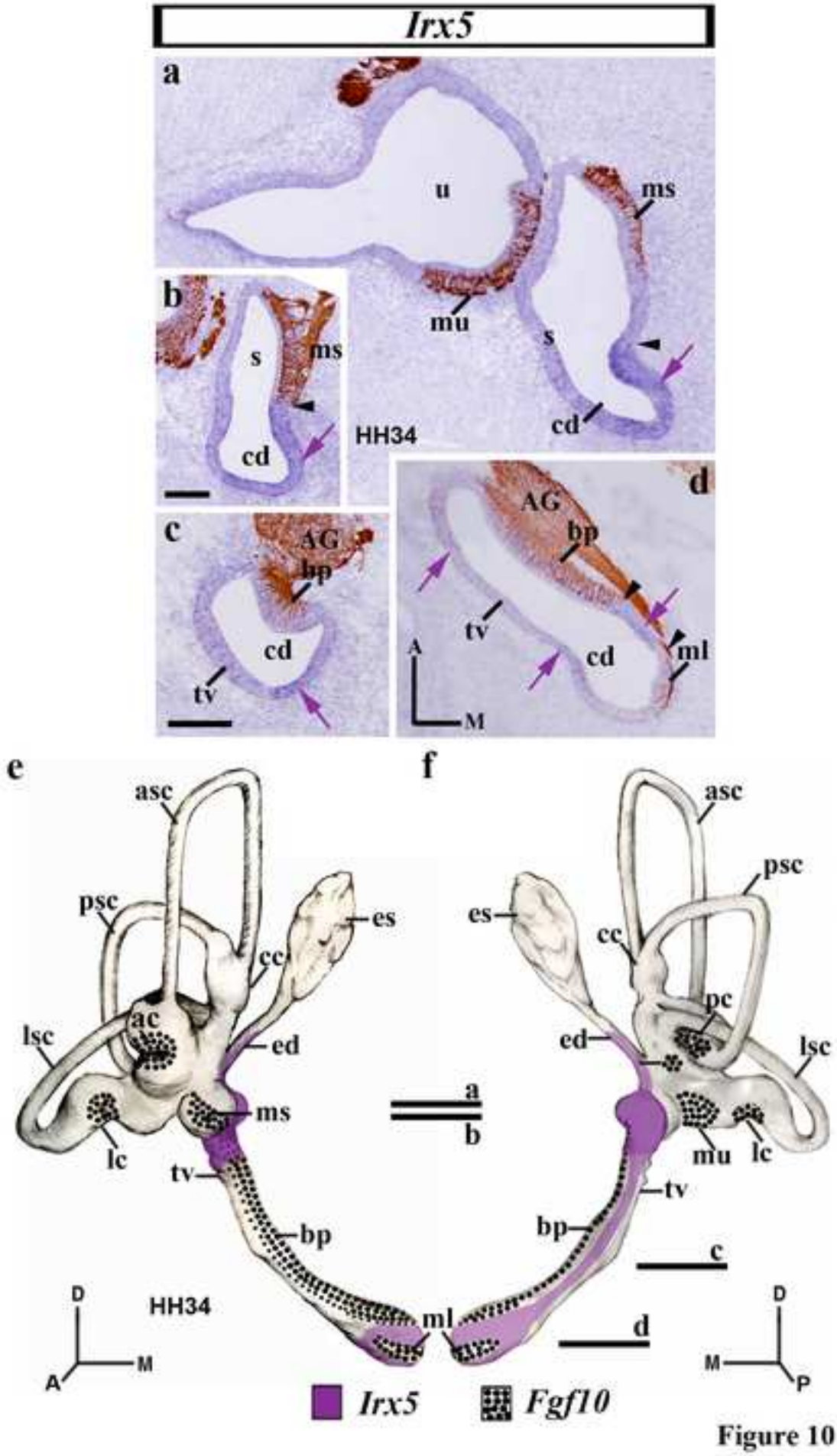
Irx5
a
u
ms
mu
s
cd
HH34
b
s
ms
cd
c
AG
bp
cd
tv
d
AG
bp
tv
cd
ml
A
M
e
asc
psc
es
cc
ac
lsc
ed
ms
lc
tv
bp
ml
HH34
D
A
M
f
asc
psc
es
cc
pc
ed
lsc
mu
lc
tv
bp
a
b
c
d
D
M
P
Irx5
Fgf10

Figure 10

Table

Gene symbol	NCBI accession no.	Size (bp)	Position	Antisense probe enzyme/polymerase	Reference/laboratory
Irx1	AJ238354	800	604-1404	Not I /T3	Unpublished data Kate G. Storey
Irx2	AJ237599	750	684-1434	EcoR I /T7	Goriely et al, 1999
Irx3	AF 157620.1	300	1-300	Hind III/ T3	Kobayashi et al, 2002
Irx4	NM 001001744.1	650	1447-2097	Not I /T3	EST clone: ChEST971m9
Irx5	M_015292371.1	323	1460-1782	Nco I/ Sp6	This work
Irx6	M_015292360.1	285	952-1236	Nco I/ Sp6	This work
Fgf10	NM_204696.1	686	214–900	Nco I/Sp6	Alsina et al., 2004

Table 1. Gene Probes Used for ISH and Their Principal Characteristics